

Isogeometric collocation on planar multi-patch domains

Mario Kapl^{a,*}, Vito Vitrih^b

^a*Johann Radon Institute for Computational and Applied Mathematics,
Austrian Academy of Sciences, Linz, Austria*

^b*IAM and FAMNIT, University of Primorska, Koper, Slovenia*

Abstract

We present an isogeometric framework based on collocation to construct a C^2 -smooth approximation of the solution of the Poisson's equation over planar bilinearly parameterized multi-patch domains. The construction of the used globally C^2 -smooth discretization space for the partial differential equation is simple and works uniformly for all possible multi-patch configurations. The basis of the C^2 -smooth space can be described as the span of three different types of locally supported functions corresponding to the single patches, edges and vertices of the multi-patch domain. For the selection of the collocation points, which is important for the stability and convergence of the collocation problem, two different choices are numerically investigated. The first approach employs the tensor-product Greville abscissae as collocation points, and shows for the multi-patch case the same convergence behavior as for the one-patch case [2], which is suboptimal in particular for odd spline degree. The second approach generalizes the concept of superconvergent points from the one-patch case (cf. [1, 15, 32]) to the multi-patch case. Again, these points possess better convergence properties than Greville abscissae in case of odd spline degree.

Keywords: isogeometric analysis; collocation; superconvergent points; second order continuity; multi-patch domain; Poisson's equation

2010 MSC: 65N35, 65D17, 68U07

1. Introduction

Isogeometric Analysis (IgA) is an approach for numerically solving a partial differential equation (PDE) by using the same spline or NURBS space for describing the geometry and for representing the solution of the considered PDE, cf. [4, 10, 18]. Usually, the developed PDE solvers are based on finding a solution of the variational (weak) form of the PDE, since using the weak form requires less smooth functions compared to directly employing the strong form. However, this technique needs the evaluation of integrals by using some particular quadrature rules, and the accuracy of the solution depends on the quality of the numerical integration. In contrast, solving the strong form of the PDE via collocation eliminates integration but requires spaces of higher regularity.

*Corresponding author

Email addresses: mario.kapl@ricam.oeaw.ac.at (Mario Kapl), vito.vitrih@upr.si (Vito Vitrih)

While in case of a one-patch domain, the higher continuity of the functions can be easily guaranteed by using spline functions with the desired smoothness within the patch, the construction of C^s -smooth ($s \geq 1$) isogeometric spline spaces over multi-patch domains is challenging, and is the task of current research, see e.g. [6–9, 20–23, 28, 29, 33, 34, 40, 41] for $s = 1$ and [24–27, 39] for $s = 2$. The design of C^s -smooth multi-patch spline spaces is linked to the concept of geometric continuity of multi-patch surfaces, cf. [17, 35], due to the fact that *an isogeometric function is C^s -smooth on a multi-patch domain if and only if its associated multi-patch graph surface is G^s -smooth*, cf. [16, 28].

So far, the problem of isogeometric collocation has been mostly explored on one-patch domains, see e.g. [1, 2, 5, 13–15, 30–32, 36, 38]. For analyzing the convergence behavior of a particular approach, the errors are generally computed with respect to L^∞ , $W^{1,\infty}$ and $W^{2,\infty}$ norm, or equivalently with respect to L^2 , H^1 and H^2 norm, respectively. The study of isogeometric collocation methods has started in [2] by using the Greville and Demko abscissae as collocation points. In comparison to the Galerkin approach, both choices show a suboptimal convergence behavior with respect to $L^2(L^\infty)$ norm, namely of orders $\mathcal{O}(h^p)$ and $\mathcal{O}(h^{p-1})$ under h -refinement for even and odd spline degree p , respectively, and additionally a suboptimal convergence order $\mathcal{O}(h^{p-1})$ with respect to $H^1(W^{1,\infty})$ norm but just in case of odd spline degree p .

In [1], an isogeometric collocation method has been presented, which is based on the computation and on the use of specific collocation points called *superconvergent points*. The proposed technique possesses only for even spline degree p in case of the $L^2(L^\infty)$ norm a suboptimal convergence behavior of order $\mathcal{O}(h^p)$, and is optimal for all other cases. This is achieved at the expense of solving an overdetermined linear system due to the fact that the number of superconvergent points is larger than the number of degrees of freedom. The two methods [15] and [32] select different specific subsets of the superconvergent points to achieve that the number of collocation points coincides with the number of degrees of freedom. While the points¹ in [15] are chosen in an alternating way, which reduces for the case of odd spline degree p the convergence order also to $\mathcal{O}(h^p)$ in the $L^2(L^\infty)$ norm, the points in [32] are selected in a clustered way to maintain the convergence behavior of [1].

In [1, 2, 14, 32, 38], the concept of isogeometric collocation has been mostly used for solving the Poisson’s equation. Further problems and PDEs of interest in the framework of isogeometric collocation are amongst others linear and nonlinear elasticity, elastostatics and elastodynamics [1, 3, 13–15, 19, 36, 38], plate/shell problems [15, 30] and beam problems [5, 31].

As already mentioned before, most of the existing isogeometric collocation methods have in common that they are mainly restricted to the case of one-patch domains. Two techniques which also deal with the case of multi-patch domains are [3, 19]. While in [3] standard NURBS functions are employed, the work in [19] is based on the use of PHT-splines [12]. Since for both methods the used spline spaces are in general just C^0 -smooth across the patch interfaces, special techniques for the collocation on the interfaces are

¹In [15], the superconvergent points are also denoted as *Cauchy Galerkin points*, since collocation at these points produces the Galerkin solution exactly.

required.

The goal of this paper is to compute a globally C^2 -smooth approximation of the solution of the Poisson's equation on planar bilinearly parameterized multi-patch domains by means of isogeometric collocation. For this purpose, a globally C^2 -smooth discretization space is generated and used. The construction of this C^2 -smooth multi-patch space is based on and extends the work [27]. There, a subspace of the entire C^2 -smooth spline space [24] has been generated, which possesses a simpler structure as the entire C^2 -smooth space but still maintains the full approximation properties. The construction of the locally supported basis functions is simple via explicit formulae or by computing the null space of a small system of linear equations. Whereas the basis construction in [27] works uniformly for all possible multi-patch configurations, the number of basis functions depends on the initial geometry. This work overcomes the latter limitation by constructing a C^2 -smooth spline space whose dimension is independent of the initial geometry by e.g. additionally enforcing that the functions have to be C^4 -smooth at the inner vertices and at the boundary vertices of patch valencies greater or equal to three of the multi-patch domain.

The generated C^2 -smooth spline space can be directly employed to perform isogeometric collocation on the multi-patch domain, and no special treatment for the patch interfaces as in [3, 19] is needed. For assembling the system matrices of the collocation problem two different choices of collocation points are studied. On the one hand, we employ the tensor-product Greville abscissae for the single patches, and on the other hand we generalize the so-called superconvergent points for the one-patch case (cf. [1, 15, 32]) to the multi-patch case. Like in the one-patch case, the superconvergent points possess a better convergence behavior as the Greville points for odd spline degree, namely of orders $\mathcal{O}(h^p)$, $\mathcal{O}(h^p)$ and $\mathcal{O}(h^{p-1})$ in comparison to $\mathcal{O}(h^{p-1})$, $\mathcal{O}(h^{p-1})$ and $\mathcal{O}(h^{p-1})$ with respect to the L^2 (L^∞), H^1 ($W^{1,\infty}$) and H^2 ($W^{2,\infty}$) norm.

The remainder of the paper is organized as follows. Section 2 presents the construction of a particular C^2 -smooth isogeometric spline space over bilinear multi-patch domains, which will be used as a discretization space for solving the Poisson's equation by means of isogeometric collocation. The multi-patch isogeometric collocation method as well as two different strategies for choosing the collocation points are described in Section 3. On the basis of several numerical examples, the convergence behavior under h -refinement of the collocation method is studied in Section 4, and demonstrates the potential of the method for the use in IgA. Finally, we conclude the paper.

2. A C^2 -smooth isogeometric spline space

The construction of a particular C^2 -smooth multi-patch isogeometric spline space will be presented, which will be based on and will extend the work [27]. The C^2 -smooth space will be used in Section 3 to build an isogeometric collocation method for solving the Poisson's equation over bilinear multi-patch domains. We will start with the introduction of the multi-patch setting, which will be used throughout the paper.

2.1. The multi-patch setting

Let \mathcal{I}_Ω be an index set, and let Ω and $\Omega^{(i)}$, $i \in \mathcal{I}_\Omega$, be open domains in \mathbb{R}^2 , such that $\overline{\Omega} = \cup_{i \in \mathcal{I}_\Omega} \overline{\Omega^{(i)}}$. Furthermore, let $\Omega^{(i)}$, $i \in \mathcal{I}_\Omega$, be quadrangular patches, which are mutually disjoint, and the closures of any two of them have either an empty intersection, possess exactly one common vertex or share the whole common edge. Additionally, the deletion of any vertex of the multi-patch domain $\overline{\Omega}$ does not split $\overline{\Omega}$ into subdomains, whose union would be unconnected. We will further assume that each patch $\overline{\Omega^{(i)}}$ is parameterized by a bilinear, bijective and regular geometry mapping $\mathbf{F}^{(i)}$,

$$\mathbf{F}^{(i)} : [0, 1]^2 \rightarrow \mathbb{R}^2, \quad \boldsymbol{\xi} = (\xi_1, \xi_2) \mapsto \mathbf{F}^{(i)}(\boldsymbol{\xi}) = \mathbf{F}^{(i)}(\xi_1, \xi_2), \quad i \in \mathcal{I}_\Omega,$$

such that $\overline{\Omega^{(i)}} = \mathbf{F}^{(i)}([0, 1]^2)$. We will also use the splitting of the multi-patch domain $\overline{\Omega}$ into the single patches $\Omega^{(i)}$, $i \in \mathcal{I}_\Omega$, edges $\Gamma^{(i)}$, $i \in \mathcal{I}_\Gamma$ and vertices $\mathbf{v}^{(i)}$, $i \in \mathcal{I}_\Xi$, i.e.

$$\overline{\Omega} = \bigcup_{i \in \mathcal{I}_\Omega} \Omega^{(i)} \dot{\cup} \bigcup_{i \in \mathcal{I}_\Gamma} \Gamma^{(i)} \dot{\cup} \bigcup_{i \in \mathcal{I}_\Xi} \mathbf{v}^{(i)},$$

where \mathcal{I}_Γ and \mathcal{I}_Ξ are the index sets of the indices of the edges $\Gamma^{(i)}$ and vertices $\mathbf{v}^{(i)}$, respectively. We further have $\mathcal{I}_\Gamma = \mathcal{I}_{\Gamma_I} \dot{\cup} \mathcal{I}_{\Gamma_B}$ and $\mathcal{I}_\Xi = \mathcal{I}_{\Xi_I} \dot{\cup} \mathcal{I}_{\Xi_B}$ with $\mathcal{I}_{\Xi_B} = \mathcal{I}_{\Xi_1} \dot{\cup} \mathcal{I}_{\Xi_2} \dot{\cup} \mathcal{I}_{\Xi_3}$, where \mathcal{I}_{Γ_I} and \mathcal{I}_{Γ_B} contain all indices of interfaces and boundary edges, respectively, \mathcal{I}_{Ξ_I} and \mathcal{I}_{Ξ_B} collect all indices of inner and boundary vertices, respectively, and \mathcal{I}_{Ξ_1} , \mathcal{I}_{Ξ_2} and \mathcal{I}_{Ξ_3} are further the index sets of the indices of boundary vertices of patch valencies one, two and greater or equal to three, respectively. In addition, the patch valency of a vertex $\mathbf{v}^{(i)}$ will be denoted by ν_i .

Let $\mathcal{S}_h^{p,r}([0, 1])$ be the univariate spline space of degree p , regularity r and mesh size $h = \frac{1}{k+1}$ on the unit interval $[0, 1]$, constructed from the uniform open knot vector

$$(t_0^{p,r}, \dots, t_{2p+k(p-r)+1}^{p,r}) = \left(\underbrace{0, \dots, 0}_{(p+1)\text{-times}}, \underbrace{\frac{1}{k+1}, \dots, \frac{1}{k+1}}_{(p-r)\text{-times}}, \dots, \underbrace{\frac{k}{k+1}, \dots, \frac{k}{k+1}}_{(p-r)\text{-times}}, \underbrace{1, \dots, 1}_{(p+1)\text{-times}} \right),$$

where k is the number of different inner knots. Furthermore, let $\mathcal{S}_h^{p,r}([0, 1]^2)$ be the tensor-product spline space $\mathcal{S}_h^{p,r}([0, 1]) \otimes \mathcal{S}_h^{p,r}([0, 1])$ on the unit-square $[0, 1]^2$. We denote the B-splines of the spaces $\mathcal{S}_h^{p,r}([0, 1])$ and $\mathcal{S}_h^{p,r}([0, 1]^2)$ by $N_j^{p,r}$ and $N_{j_1, j_2}^{p,r} = N_{j_1}^{p,r} N_{j_2}^{p,r}$, respectively, with $j, j_1, j_2 = 0, 1, \dots, n-1$, and $n = p+1+k(p-r)$. We assume that $p \geq 5$, $2 \leq r \leq p-3$, and that the number of inner knots satisfies $k \geq \frac{9-p}{p-r-2}$. These assumptions are necessary to ensure that the constructed C^2 -smooth spline spaces in Section 2.3 will be h -refineable and well-defined, see also [26, 27]. Since the geometry mappings $\mathbf{F}^{(i)}$, $i \in \mathcal{I}_\Omega$, are bilinearly parameterized, we trivially have that

$$\mathbf{F}^{(i)} \in \mathcal{S}_h^{p,r}([0, 1]^2) \times \mathcal{S}_h^{p,r}([0, 1]^2).$$

Moreover, we assume for two neighboring patches $\Omega^{(i_0)}$ and $\Omega^{(i_1)}$ with the common interface $\Gamma^{(i)} \subset \overline{\Omega^{(i_0)}} \cap \overline{\Omega^{(i_1)}}$ that the associated geometry mappings $\mathbf{F}^{(i_0)}$ and $\mathbf{F}^{(i_1)}$ are parameterized as given in Fig. 1 (left), and assume for the neighboring patches enclosing

an inner or boundary vertex $\mathbf{v}^{(i)}$ of patch valency $\nu_i \geq 3$ that the associated geometry mappings are parameterized as shown in Fig. 1 (right). For the latter case, we additionally assume that the patches enclosing the vertex $\mathbf{v}^{(i)}$ are relabeled by $\Omega^{(i_0)}, \dots, \Omega^{(i_{\nu_i-1})}$, and that the common interfaces² of the two-patch subdomains $\overline{\Omega^{(i_\ell)}} \cup \overline{\Omega^{(i_{\ell+1})}}$, $\ell = 0, 1, \dots, \nu_i - 1$, are relabeled by $\Gamma^{(i_{\ell+1})}$. In case of an inner vertex $\mathbf{v}^{(i)}$ we further consider the lower index ℓ of the indices i_ℓ modulo ν_i , which just means that the lower index ℓ is replaced by the remainder of the division of ℓ by ν_i . Note that the local reparameterizations as shown in Fig. 1 are always possible (if necessary), and hence can be assumed to be satisfied without loss of generality.

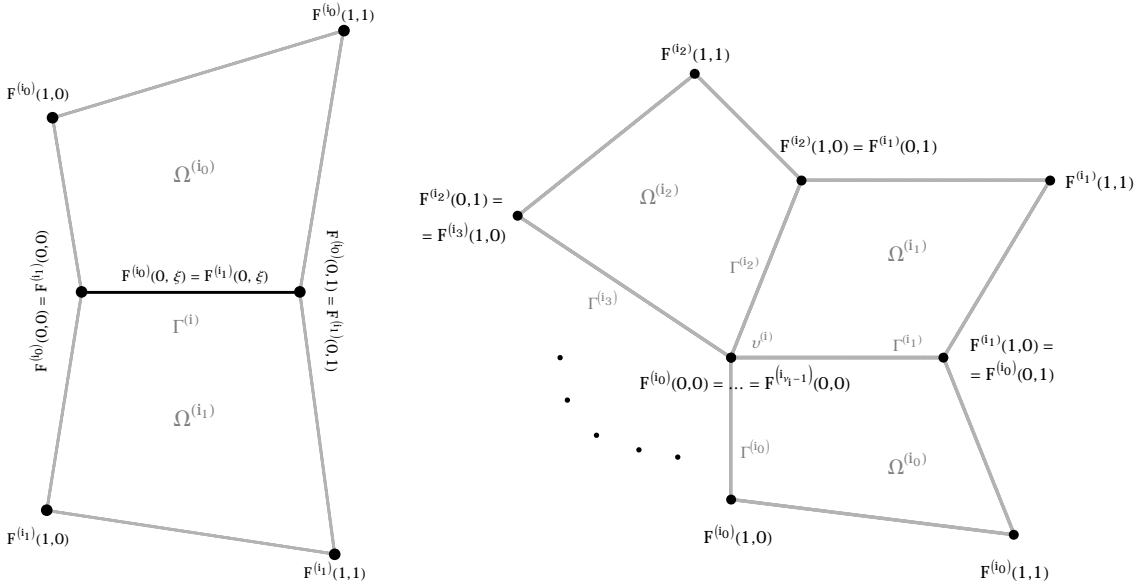


Figure 1: Left: Considering two neighboring patches $\Omega^{(i_0)}$ and $\Omega^{(i_1)}$, we can always assume that the two corresponding geometry mappings $\mathbf{F}^{(i_0)}$ and $\mathbf{F}^{(i_1)}$ are parameterized as shown. Right: For the patches $\Omega^{(i_\ell)}$, $\ell = 0, 1, \dots, \nu_i - 1$, which enclose the vertex $\mathbf{v}^{(i)}$, the corresponding geometry mappings $\mathbf{F}^{(i_\ell)}$ can be always reparameterized to be given as visualized.

2.2. C^2 -smoothness across patch interfaces

The space of C^2 -smooth isogeometric functions on Ω is given as

$$\mathcal{V} = \left\{ \phi \in C^2(\overline{\Omega}) : \phi|_{\overline{\Omega^{(i)}}} \in \mathcal{S}_h^{p,r}([0,1]^2) \circ (\mathbf{F}^{(i)})^{-1}, i \in \mathcal{I}_\Omega \right\}.$$

This space can be characterized by means of the concept of geometric continuity of multi-patch surfaces, cf. [17, 35]. *An isogeometric function ϕ belongs to the space \mathcal{V} if and only if for any two neighboring patches $\Omega^{(i_0)}$ and $\Omega^{(i_1)}$ with the common interface $\overline{\Gamma^{(i)}} = \overline{\Omega^{(i_0)}} \cap \overline{\Omega^{(i_1)}}$, $i \in \mathcal{I}_{\Gamma}$, the associated graph surface patches $\begin{bmatrix} \mathbf{F}^{(i_0)} \\ \phi \circ \mathbf{F}^{(i_0)} \end{bmatrix}$ and $\begin{bmatrix} \mathbf{F}^{(i_1)} \\ \phi \circ \mathbf{F}^{(i_1)} \end{bmatrix}$*

²In case of a boundary vertex $\mathbf{v}^{(i)}$, we denote the boundary edges by $\Gamma^{(i_0)}$ and $\Gamma^{(i_{\nu_i})}$.

are G^2 -smooth across their common interface, see e.g. [16, 28]. An equivalent condition to the G^2 -smoothness of the two neighboring graph surface patches is that the two associated spline functions $g^{(i_0)} = \phi \circ \mathbf{F}^{(i_0)}$ and $g^{(i_1)} = \phi \circ \mathbf{F}^{(i_1)}$ satisfy

$$\underbrace{g^{(i_0)}(0, \xi) = g^{(i_1)}(0, \xi)}_{:=g_0(\xi)}, \quad (1)$$

$$\underbrace{\frac{D_{\xi_2} g^{(i_0)}(0, \xi) - \beta_{\Gamma^{(i_0)}}^{(i_0)}(\xi) g_0'(\xi)}{\alpha_{\Gamma^{(i_0)}}^{(i_0)}(\xi)} = \frac{D_{\xi_2} g^{(i_1)}(0, \xi) - \beta_{\Gamma^{(i_1)}}^{(i_1)}(\xi) g_0'(\xi)}{\alpha_{\Gamma^{(i_1)}}^{(i_1)}(\xi)}}_{:=g_1(\xi)}, \quad (2)$$

and

$$\frac{D_{\xi_1 \xi_1} g^{(i_0)}(0, \xi) - (\beta_{\Gamma^{(i_0)}}^{(i_0)}(\xi))^2 g_0''(\xi) - 2\alpha_{\Gamma^{(i_0)}}^{(i_0)} \beta_{\Gamma^{(i_0)}}^{(i_0)}(\xi) g_1'(\xi)}{(\alpha_{\Gamma^{(i_0)}}^{(i_0)}(\xi))^2} = \frac{D_{\xi_1 \xi_1} g^{(i_1)}(0, \xi) - (\beta_{\Gamma^{(i_1)}}^{(i_1)}(\xi))^2 g_0''(\xi) - 2\alpha_{\Gamma^{(i_1)}}^{(i_1)} \beta_{\Gamma^{(i_1)}}^{(i_1)}(\xi) g_1'(\xi)}{(\alpha_{\Gamma^{(i_1)}}^{(i_1)}(\xi))^2}, \quad (3)$$

for all $\xi \in [0, 1]$, cf. [26, Lemma 1], where $\alpha_{\Gamma^{(i)}}^{(\tau)}$ and $\beta_{\Gamma^{(i)}}^{(\tau)}$, $\tau \in \{i_0, i_1\}$, are linear polynomials given by

$$\alpha_{\Gamma^{(i)}}^{(\tau)}(\xi) = c_1 \det[D_{\xi_1} \mathbf{F}^{(\tau)}(0, \xi), D_{\xi_2} \mathbf{F}^{(\tau)}(0, \xi)],$$

and

$$\beta_{\Gamma^{(i)}}^{(\tau)}(\xi) = \frac{D_{\xi_1} \mathbf{F}^{(\tau)}(0, \xi) \cdot D_{\xi_2} \mathbf{F}^{(\tau)}(0, \xi)}{\|D_{\xi_2} \mathbf{F}^{(\tau)}(0, \xi)\|^2},$$

respectively, with $c_1 \in \mathbb{R}$ such that

$$\|\alpha_{\Gamma^{(i_0)}}^{(i_0)} + 1\|_{L^2}^2 + \|\alpha_{\Gamma^{(i_1)}}^{(i_1)} - 1\|_{L^2}^2$$

is minimized, cf. [27]. Note that $\alpha_{\Gamma^{(i_0)}}^{(i_0)} < 0$ and $\alpha_{\Gamma^{(i_1)}}^{(i_1)} > 0$, since the geometry mappings $\mathbf{F}^{(i_0)}$ and $\mathbf{F}^{(i_1)}$ are regular.

The space \mathcal{V} has been studied in different configurations in [24–26]. There, it has been observed that the space \mathcal{V} possesses a complex structure and its dimension depends on the initial geometry. In the next subsection, we will consider instead a subspace of the space \mathcal{V} , whose structure is simpler and whose dimension is independent of the initial geometry.

2.3. A C^2 -smooth isogeometric space

We will describe the construction of a particular C^2 -smooth space $\mathcal{W} \subseteq \mathcal{V}$, which will be similar to the one in [27]. There will be two main differences between the newly constructed space \mathcal{W} and the space from [27]. Firstly, the space \mathcal{W} will not be anymore restricted to containing just C^2 -smooth functions fulfilling the homogeneous boundary conditions of order 2 given by

$$u(\mathbf{x}) = \frac{\partial u}{\partial \mathbf{n}}(\mathbf{x}) = \Delta u(\mathbf{x}) = 0, \quad \mathbf{x} \in \partial\Omega,$$

which have been used in [27] as boundary conditions for solving the triharmonic equation via its weak form and standard Galerkin discretization. Secondly, the dimension of the space \mathcal{W} will now be independent of the initial geometry.

Analogous to [27], the space \mathcal{W} is defined as the direct sum

$$\mathcal{W} = \left(\bigoplus_{i \in \mathcal{I}_\Omega} \mathcal{W}_{\Omega^{(i)}} \right) \oplus \left(\bigoplus_{i \in \mathcal{I}_\Gamma} \mathcal{W}_{\Gamma^{(i)}} \right) \oplus \left(\bigoplus_{i \in \mathcal{I}_\Xi} \mathcal{W}_{\mathbf{v}^{(i)}} \right), \quad (4)$$

where $\mathcal{W}_{\Omega^{(i)}}$, $\mathcal{W}_{\Gamma^{(i)}}$ and $\mathcal{W}_{\mathbf{v}^{(i)}}$ are subspaces corresponding to the single patches $\Omega^{(i)}$, edges $\Gamma^{(i)}$ and vertices $\mathbf{v}^{(i)}$, respectively. While the construction of the subspaces $\mathcal{W}_{\Omega^{(i)}}$ and $\mathcal{W}_{\Gamma^{(i)}}$ will work analogously to or similar as in [27], and hence will be kept short below, the construction of the subspaces $\mathcal{W}_{\mathbf{v}^{(i)}}$ will differ.

2.3.1. The patch subspace $\mathcal{W}_{\Omega^{(i)}}$ and the edge subspace $\mathcal{W}_{\Gamma^{(i)}}$

As in [27], the patch subspaces $\mathcal{W}_{\Omega^{(i)}}$, $i \in \mathcal{I}_\Omega$, are given as

$$\mathcal{W}_{\Omega^{(i)}} = \text{span}\{\phi_{\Omega^{(i)};j_1,j_2} \mid j_1, j_2 = 3, 4, \dots, n-4\},$$

with the functions

$$\phi_{\Omega^{(i)};j_1,j_2}(\mathbf{x}) = \begin{cases} (N_{j_1,j_2}^{\mathbf{p},\mathbf{r}} \circ (\mathbf{F}^{(i)})^{-1})(\mathbf{x}) & \text{if } \mathbf{x} \in \Omega^{(i)}, \\ 0 & \text{otherwise.} \end{cases} \quad (5)$$

For the edge subspaces $\mathcal{W}_{\Gamma^{(i)}}$, $i \in \mathcal{I}_\Gamma$, we have to distinguish between the case of a boundary edge $\Gamma^{(i)}$, i.e. $i \in \mathcal{I}_{\Gamma_B}$, and the case of an interface $\Gamma^{(i)}$, $i \in \mathcal{I}_{\Gamma_I}$. Let us start with the case of a boundary edge $\Gamma^{(i)}$, $i \in \mathcal{I}_{\Gamma_B}$. Assume without loss of generality, that the boundary edge $\Gamma^{(i)}$ is contained in the geometry mapping $\mathbf{F}^{(i_0)}$ and is given by $\mathbf{F}^{(i_0)}(\{0\} \times (0, 1))$. Then the subspace $\mathcal{W}_{\Gamma^{(i)}}$ possesses the form

$$\mathcal{W}_{\Gamma^{(i)}} = \text{span}\{\phi_{\Gamma_B^{(i)};j_1,j_2} \mid j_2 = 5 - j_1, \dots, n + j_1 - 6, j_1 = 0, 1, 2\},$$

where $\phi_{\Gamma_B^{(i)};j_1,j_2}$ is defined similar to (5) as

$$\phi_{\Gamma_B^{(i)};j_1,j_2}(\mathbf{x}) = \begin{cases} (N_{j_1,j_2}^{\mathbf{p},\mathbf{r}} \circ (\mathbf{F}^{(i_0)})^{-1})(\mathbf{x}) & \text{if } \mathbf{x} \in \overline{\Omega^{(i_0)}}, \\ 0 & \text{otherwise.} \end{cases} \quad (6)$$

In case of an interface $\Gamma^{(i)} \subset \overline{\Omega^{(i_0)}} \cap \overline{\Omega^{(i_1)}}$, $i \in \mathcal{I}_{\Gamma_I}$, and assuming without loss of generality that the associated geometry mappings $\mathbf{F}^{(i_0)}$ and $\mathbf{F}^{(i_1)}$ are parameterized as in Fig. 1 (left), the edge subspace $\mathcal{W}_{\Gamma^{(i)}}$ is defined as

$$\mathcal{W}_{\Gamma^{(i)}} = \text{span}\{\phi_{\Gamma_I^{(i)};j_1,j_2} \mid j_2 = 5 - j_1, \dots, n_{j_1} + j_1 - 6, j_1 = 0, 1, 2\},$$

with the functions

$$\phi_{\Gamma_I^{(i)};j_1,j_2}(\mathbf{x}) = \begin{cases} (g_{\Gamma^{(i)};j_1,j_2}^{(i_0)} \circ (\mathbf{F}^{(i_0)})^{-1})(\mathbf{x}) & \text{if } \mathbf{x} \in \overline{\Omega^{(i_0)}}, \\ (g_{\Gamma^{(i)};j_1,j_2}^{(i_1)} \circ (\mathbf{F}^{(i_1)})^{-1})(\mathbf{x}) & \text{if } \mathbf{x} \in \overline{\Omega^{(i_1)}}, \end{cases} \quad (7)$$

where

$$\begin{aligned}
g_{\Gamma^{(i)};0,j_2}^{(\tau)}(\xi_1, \xi_2) &= N_{j_2}^{p,r+2}(\xi_2)M_0(\xi_1) + \beta_{\Gamma^{(i)}}^{(\tau)}(\xi_2)(N_{j_2}^{p,r+2})'(\xi_2)M_1(\xi_1) \\
&\quad + \left(\beta_{\Gamma^{(i)}}^{(\tau)}(\xi_2)\right)^2 (N_{j_2}^{p,r+2})''(\xi_2)M_2(\xi_1), \\
g_{\Gamma^{(i)};1,j_2}^{(\tau)}(\xi_1, \xi_2) &= \frac{p}{h} \left(\alpha_{\Gamma^{(i)}}^{(\tau)}(\xi_2)N_{j_2}^{p-1,r+1}(\xi_2)M_1(\xi_1) \right. \\
&\quad \left. + 2\alpha_{\Gamma^{(i)}}^{(\tau)}(\xi_2)\beta_{\Gamma^{(i)}}^{(\tau)}(\xi_2)(N_{j_2}^{p-1,r+1})'(\xi_2)M_2(\xi_1)\right), \\
g_{\Gamma^{(i)};2,j_2}^{(\tau)}(\xi_1, \xi_2) &= \frac{p(p-1)}{h^2} \left(\alpha_{\Gamma^{(i)}}^{(\tau)}(\xi_2)\right)^2 N_{j_2}^{p-2,r}(\xi_2)M_2(\xi_1),
\end{aligned} \tag{8}$$

for $\tau \in \{i_0, i_1\}$, with

$$M_0(\xi) = \sum_{j=0}^2 N_j^{p,r}(\xi), \quad M_1(\xi) = \frac{p}{h} (N_1^{p,r}(\xi) + 2N_2^{p,r}(\xi)), \quad M_2(\xi) = \frac{p(p-1)}{h^2} N_2^{p,r}(\xi),$$

and

$$n_0 = \dim(\mathcal{S}_h^{p,r+2}([0,1])), \quad n_1 = \dim(\mathcal{S}_h^{p-1,r+1}([0,1])), \quad n_2 = \dim(\mathcal{S}_h^{p-2,r}([0,1])).$$

All functions of the patch subspaces $\mathcal{W}_{\Omega^{(i)}}$, $i \in \mathcal{I}_{\Omega}$, and of the edge subspaces $\mathcal{W}_{\Gamma^{(i)}}$, $i \in \mathcal{I}_{\Gamma}$, are C^2 -smooth on $\overline{\Omega}$, since the Eqs. (1)–(3) are satisfied for all interfaces $\overline{\Gamma^{(j)}}$, $j \in \mathcal{I}_{\Gamma}$. In case of the patch subspaces $\mathcal{W}_{\Omega^{(i)}}$ and of the edge subspaces $\mathcal{W}_{\Gamma^{(i)}}$ for $i \in \mathcal{I}_{\Gamma_B}$, the equations are even trivially satisfied, since the functions have vanishing values, gradients and Hessians on all interfaces $\overline{\Gamma^{(j)}}$, $j \in \mathcal{I}_{\Gamma_I}$. In case of the edge subspaces $\mathcal{W}_{\Gamma^{(i)}}$ for $i \in \mathcal{I}_{\Gamma_I}$, whereas the equations are also trivially fulfilled for the interfaces $\overline{\Gamma^{(j)}}$, $j \in \mathcal{I}_{\Gamma} \setminus \{i\}$, the particular construction of the functions $\phi_{\Gamma_I^{(i)};j_1,j_2}$ ensures that the Eqs. (1)–(3) are satisfied for the non-trivial case of the corresponding interface $\overline{\Gamma^{(i)}}$, too, cf. [26, 27].

2.3.2. The vertex subspace $\mathcal{W}_{\mathbf{v}^{(i)}}$

The vertex subspaces $\mathcal{W}_{\mathbf{v}^{(i)}}$, $i \in \mathcal{I}_{\Xi}$, constructed in this work, will differ from the ones in [27]. The new construction of the subspaces will ensure that the dimension of the vertex subspaces will now be independent of the initial geometry. Furthermore, the design of the vertex subspaces $\mathcal{W}_{\mathbf{v}^{(i)}}$, $i \in \mathcal{I}_{\Xi_B}$, will not be anymore restricted to any boundary conditions. We will distinguish between four cases, namely if the vertex $\mathbf{v}^{(i)}$ is an inner vertex, i.e. $i \in \mathcal{I}_{\Xi_I}$, a boundary vertex of patch valency one, i.e. $i \in \mathcal{I}_{\Xi_1}$, a boundary vertex of patch valency two, i.e. $i \in \mathcal{I}_{\Xi_2}$, or a boundary vertex of patch valency greater or equal to three, i.e. $i \in \mathcal{I}_{\Xi_3}$.

Let us start with the case of an inner vertex $\mathbf{v}^{(i)}$, that is $i \in \mathcal{I}_{\Xi_I}$. Recall that we assume without loss of generality that the geometry mappings $\mathbf{F}^{(i_\ell)}$ containing the vertex $\mathbf{v}^{(i)}$ are relabeled and parameterized as described and shown in Section 2.1 and Fig. 1 (right), respectively. Again, the lower index ℓ of the indices i_ℓ will be considered modulo ν_i . First

of all, we consider analogous to [27], the isogeometric function $\phi_{\mathbf{v}^{(i)}} : \Omega \rightarrow \mathbb{R}$, which is defined as

$$\phi_{\mathbf{v}^{(i)}}(\mathbf{x}) = \begin{cases} (g_{i_\ell} \circ (\mathbf{F}^{(i_\ell)})^{-1})(\mathbf{x}) & \text{if } \mathbf{x} \in \overline{\Omega^{(i_\ell)}}, \ell = 0, 1, \dots, \nu_i - 1, \\ 0 & \text{otherwise,} \end{cases} \quad (9)$$

where the functions g_{i_ℓ} are given as

$$\begin{aligned} g_{i_\ell}(\xi_1, \xi_2) &= \underbrace{\sum_{j_1=0}^2 \sum_{j_2=0}^{4-j_1} a_{j_1, j_2}^{\Gamma^{(i_\ell)}} g_{\Gamma^{(i_\ell)}; j_1, j_2}^{(i_\ell)}(\xi_2, \xi_1)}_{:=g_{i_\ell}^{\Gamma^{(i_\ell)}}(\xi_1, \xi_2)} + \underbrace{\sum_{j_1=0}^2 \sum_{j_2=0}^{4-j_1} a_{j_1, j_2}^{\Gamma^{(i_{\ell+1})}} g_{\Gamma^{(i_{\ell+1})}; j_1, j_2}^{(i_\ell)}(\xi_1, \xi_2)}_{:=g_{i_\ell}^{\Gamma^{(i_{\ell+1})}}(\xi_1, \xi_2)} - \\ &\quad \underbrace{\sum_{j_1=0}^2 \sum_{j_2=0}^2 a_{j_1, j_2}^{(i_\ell)} N_{j_1, j_2}^{\mathbf{p}, \mathbf{r}}(\xi_1, \xi_2)}_{:=g_{i_\ell}^{\Omega^{(i_\ell)}}(\xi_1, \xi_2)}, \end{aligned} \quad (10)$$

with coefficients $a_{j_1, j_2}^{\Gamma^{(i_\ell)}}, a_{j_1, j_2}^{(i_\ell)} \in \mathbb{R}$, and with the functions $g_{\Gamma^{(i_\ell)}; j_1, j_2}^{(i_\ell)}$ and $g_{\Gamma^{(i_{\ell+1})}; j_1, j_2}^{(i_\ell)}$ given by (8).

In [27, Lemma 3], it was shown, that the function $\phi_{\mathbf{v}^{(i)}}$ is C^2 -smooth on $\overline{\Omega}$ if the coefficients $a_{j_1, j_2}^{\Gamma^{(i_\ell)}}$ and $a_{j_1, j_2}^{(i_\ell)}$ are selected in such a way that the following homogeneous linear system

$$\partial_{\xi_1}^i \partial_{\xi_2}^j \left(g_{i_\ell}^{\Gamma^{(i_{\ell+1})}} - g_{i_\ell}^{(i_\ell)} \right) (\mathbf{0}) = 0 \quad \text{and} \quad \partial_{\xi_1}^i \partial_{\xi_2}^j \left(g_{i_\ell}^{\Gamma^{(i_{\ell+1})}} - g_{i_\ell}^{\Omega^{(i_\ell)}} \right) (\mathbf{0}) = 0, \quad (11)$$

with $0 \leq i, j \leq 2$ and $\ell = 0, 1, \dots, \nu_i - 1$, is satisfied. The construction of a C^2 -smooth isogeometric function $\phi_{\mathbf{v}^{(i)}}$ is based on the idea of generating the spline function $g_{i_\ell} = \phi_{\mathbf{v}^{(i)}} \circ \mathbf{F}^{(i_\ell)}$ for each patch $\overline{\Omega^{(i_\ell)}}$, $\ell = 0, \dots, \nu_i - 1$, by using appropriate linear combinations of functions $g_{\Gamma^{(i_\ell)}; j_1, j_2}^{(i_\ell)}$ and $g_{\Gamma^{(i_{\ell+1})}; j_1, j_2}^{(i_\ell)}$, $j_1 = 0, 1, 2$, $j_2 = 0, 1, \dots, 4 - j_1$, to ensure C^2 -smoothness across the interfaces $\Gamma^{(i_\ell)}$ and $\Gamma^{(i_{\ell+1})}$, respectively, and by subtracting a linear combination of those standard B-splines $N_{j_1, j_2}^{\mathbf{p}, \mathbf{r}}$, $j_1, j_2 = 0, 1, 2$, which have been added twice, to get a well defined C^2 -smooth function $\phi_{\mathbf{v}^{(i)}}$, cf. [27, Section 4.4].

In [27], the vertex subspace $\mathcal{W}_{\mathbf{v}^{(i)}}$ has been defined as the span of all functions (9) whose spline functions g_{i_ℓ} fulfill the homogeneous linear system (11). A drawback of the resulting space is its geometry-dependent dimension. Below, we will construct a vertex subspace $\mathcal{W}_{\mathbf{v}^{(i)}}$, whose dimension will be independent of the initial geometry. This will be achieved by additionally enforcing that the functions of the generated space $\mathcal{W}_{\mathbf{v}^{(i)}}$ have to be C^4 -smooth at the vertex $\mathbf{v}^{(i)}$. This strategy can be seen as an extension of approach [23], where C^1 -smooth functions have been generated in the vicinity of a vertex $\mathbf{v}^{(i)}$ by additionally enforcing C^2 -smoothness of the functions at the vertex.

Let $\psi_{j_1, j_2} : \overline{\Omega} \rightarrow \mathbb{R}$, $j_1, j_2 = 0, \dots, 4$ with $j_1 + j_2 \leq 4$ be functions which are C^2 -smooth on $\overline{\Omega}$ and even C^4 -smooth at the vertex $\mathbf{v}^{(i)}$ such that

$$\partial_{x_1}^{m_1} \partial_{x_2}^{m_2} \psi_{j_1, j_2}(\mathbf{v}^{(i)}) = \sigma^{j_1 + j_2} \delta_{j_1}^{m_1} \delta_{j_2}^{m_2},$$

where δ_j^m is the Kronecker delta, and σ is a scaling factor given by

$$\sigma = \left(\frac{h}{p \nu_i} \sum_{\ell=0}^{\nu_i-1} \|\nabla \mathbf{F}^{(i_\ell)}(\mathbf{0})\| \right)^{-1},$$

cf. [23, Definition 14]. We define the isogeometric function $\phi_{\mathbf{v}_I^{(i)};j_1,j_2}$, $j_1, j_2 = 0, 1, \dots, 4$, $j_1 + j_2 \leq 4$, as

$$\phi_{\mathbf{v}_I^{(i)};j_1,j_2}(\mathbf{x}) = \phi_{\mathbf{v}^{(i)}}(\mathbf{x}), \quad (12)$$

where the function $\phi_{\mathbf{v}^{(i)}}$ is specified by fulfilling the interpolation conditions

$$\partial_{x_1}^{m_1} \partial_{x_2}^{m_2} \phi_{\mathbf{v}^{(i)}}(\mathbf{v}^{(i)}) = \partial_{x_1}^{m_1} \partial_{x_2}^{m_2} \psi_{j_1,j_2}(\mathbf{v}^{(i)}), \quad m_1, m_2 = 0, 1, \dots, 4, \quad m_1 + m_2 \leq 4. \quad (13)$$

The coefficients $a_{j_1,j_2}^{\Gamma^{(i_\ell)}}$ and $a_{j_1,j_2}^{(i_\ell)}$ of the spline functions g_{i_ℓ} of the isogeometric function $\phi_{\mathbf{v}_I^{(i)};j_1,j_2}$ are uniquely determined by the conditions (13), and can be computed via the following equivalent interpolation problem

$$\begin{aligned} \partial_{\xi_1}^{m_1} \partial_{\xi_2}^{m_2} g_{i_\ell}^{\Gamma^{(i_\ell)}}(\mathbf{0}) &= \partial_{\xi_1}^{m_1} \partial_{\xi_2}^{m_2} \left(\psi_{j_1,j_2} \circ \mathbf{F}^{(i_\ell)} \right)(\mathbf{0}), \quad 0 \leq m_1 \leq 4, \quad 0 \leq m_2 \leq 2, \quad m_1 + m_2 \leq 4, \\ \partial_{\xi_1}^{m_1} \partial_{\xi_2}^{m_2} g_{i_\ell}^{\Omega^{(i_\ell)}}(\mathbf{0}) &= \partial_{\xi_1}^{m_1} \partial_{\xi_2}^{m_2} \left(\psi_{j_1,j_2} \circ \mathbf{F}^{(i_\ell)} \right)(\mathbf{0}), \quad 0 \leq m_1, m_2 \leq 2, \end{aligned} \quad (14)$$

for $\ell = 0, 1, \dots, \nu_i - 1$. The presented construction of the isogeometric function $\phi_{\mathbf{v}_I^{(i)};j_1,j_2}$ works and leads to a well-defined C^2 -smooth function on $\bar{\Omega}$, which is additionally C^4 -smooth at the vertex $\mathbf{v}^{(i)}$. This is true because of the following four reasons: First, since the functions $g_{\Gamma^{(i_\ell)};0,j_2}^{(i_\ell)}$, $j_2 = 0, 1, \dots, 4$, $g_{\Gamma^{(i_\ell)};1,j_2}^{(i_\ell)}$, $j_2 = 0, 1, 2, 3$, and $g_{\Gamma^{(i_\ell)};2,j_2}^{(i_\ell)}$, $j_2 = 0, 1, 2$, of $g_{i_\ell}^{\Gamma^{(i_\ell)}}$ interpolate the traces of the form $N_{j_2}^{p,r+2}$, the first derivatives of the form $N_{j_2}^{p-1,r+1}$ and the second derivatives of the form $N_{j_2}^{p-2}$, respectively, across the interface $\Gamma^{(i_\ell)}$, cf. [26, Section 7], the first set of interpolation conditions in (14) uniquely determine all coefficients $a_{j_1,j_2}^{\Gamma^{(i_\ell)}}$. Moreover, as the functions $g_{i_\ell}^{\Gamma^{(i_\ell)}}$ ensure C^2 -smoothness across the interfaces $\Gamma^{(i_\ell)}$, we also obtain

$$\partial_{\xi_1}^{m_1} \partial_{\xi_2}^{m_2} g_{i_\ell}^{\Gamma^{(i_{\ell+1})}}(\mathbf{0}) = \partial_{\xi_1}^{m_1} \partial_{\xi_2}^{m_2} \left(\psi_{j_1,j_2} \circ \mathbf{F}^{(i_\ell)} \right)(\mathbf{0}), \quad (15)$$

for $0 \leq m_1 \leq 2$, $0 \leq m_2 \leq 4$, $m_1 + m_2 \leq 4$ and $\ell = 0, 1, \dots, \nu_i - 1$. Second, all coefficients $a_{j_1,j_2}^{(i_\ell)}$ are specified by the second set of interpolation conditions in (14). Third, thanks to the fulfillment of conditions (14) and (15) and the fact that the function g_{i_ℓ} is given by (10), we get

$$\partial_{\xi_1}^{m_1} \partial_{\xi_2}^{m_2} g_{i_\ell}(\mathbf{0}) = \partial_{\xi_1}^{m_1} \partial_{\xi_2}^{m_2} \left(\psi_{j_1,j_2} \circ \mathbf{F}^{(i_\ell)} \right)(\mathbf{0}),$$

for $0 \leq m_1 \leq 4$, $0 \leq m_2 \leq 4$, $m_1 + m_2 \leq 4$ and $\ell = 0, 1, \dots, \nu_i - 1$, which is further equivalent to satisfying conditions (13). Moreover, we obtain that the function $\phi_{\mathbf{v}_I^{(i)};j_1,j_2}$ is well defined and C^2 -smooth on $\bar{\Omega}$, where the latter property is the direct consequence of satisfying the homogeneous linear system (11). Fourth, the C^4 -smoothness of the function $\phi_{\mathbf{v}_I^{(i)};j_1,j_2}$ at vertex $\mathbf{v}^{(i)}$ follows directly from the fulfillment of the interpolation conditions (13).

Finally, we define for each inner vertex $\mathbf{v}^{(i)}$, i.e. $i \in \mathcal{I}_{\Xi_I}$, the vertex subspace $\mathcal{W}_{\mathbf{v}^{(i)}}$ as

$$\mathcal{W}_{\mathbf{v}^{(i)}} = \text{span}\{\phi_{\mathbf{v}_I^{(i)};j_1,j_2} \mid j_1, j_2 = 0, 1, \dots, 4, j_1 + j_2 \leq 4\}.$$

Let us continue with the case of a boundary vertex $\mathbf{v}^{(i)}$ of patch valency $\nu_i \geq 3$, that is $i \in \mathcal{I}_{\Xi_3}$. This can be treated similarly to the case of an inner vertex as above. The vertex subspaces $\mathcal{W}_{\mathbf{v}^{(i)}}$, $i \in \mathcal{I}_{\Xi_3}$, are defined as

$$\mathcal{W}_{\mathbf{v}^{(i)}} = \text{span}\{\phi_{\mathbf{v}_3^{(i)};j_1,j_2} \mid j_1, j_2 = 0, 1, \dots, 4, j_1 + j_2 \leq 4\},$$

where the functions $\phi_{\mathbf{v}_3^{(i)};j_1,j_2}$ are again determined just via

$$\phi_{\mathbf{v}_3^{(i)};j_1,j_2}(\mathbf{x}) = \phi_{\mathbf{v}^{(i)}}(\mathbf{x}), \quad (16)$$

by interpolating the conditions (13). The only two differences in the construction of the functions are that the lower index ℓ of the indices i_ℓ is not taken modulo ν_i , and that for the patches $\Omega^{(i_0)}$ and $\Omega^{(i_{\ell-1})}$ the functions $g_{\Gamma^{(i_0)};j_1,j_2}^{(i_0)}$ and $g_{\Gamma^{(i_{\nu_i-1})};j_1,j_2}^{(i_{\nu_i-1})}$ in (10), which are given on the boundary edges $\Gamma^{(i_0)}$ or $\Gamma^{(i_{\nu_i})}$, are just defined as standard B-splines, i.e.

$$g_{\Gamma^{(i_0)};j_1,j_2}^{(i_0)}(\xi_2, \xi_1) = N_{j_1,j_2}^{\mathbf{p},\mathbf{r}}(\xi_2, \xi_1) \quad \text{and} \quad g_{\Gamma^{(i_{\nu_i})};j_1,j_2}^{(i_{\nu_i-1})}(\xi_1, \xi_2) = N_{j_1,j_2}^{\mathbf{p},\mathbf{r}}(\xi_1, \xi_2).$$

Analogously to the case of an inner vertex, one can argue that the functions $\phi_{\mathbf{v}_3^{(i)};j_1,j_2}$ are C^2 -smooth on $\bar{\Omega}$ and even C^4 -smooth at the vertex $\mathbf{v}^{(i)}$.

In case of a boundary vertex $\mathbf{v}^{(i)}$ of patch valency $\nu_i = 2$, i.e. $i \in \mathcal{I}_{\Xi_2}$, we assume for the two neighboring patches $\Omega^{(i_0)}$ and $\Omega^{(i_1)}$ enclosing the vertex $\mathbf{v}^{(i)}$, that the corresponding geometry mappings $\mathbf{F}^{(i_0)}$ and $\mathbf{F}^{(i_1)}$ are parameterized as shown in Fig. 1 (left), that we have $\mathbf{v}^{(i)} = \mathbf{F}^{(i_0)}(\mathbf{0}) = \mathbf{F}^{(i_1)}(\mathbf{0})$, and that the common interface is denoted by $\Gamma^{(j_0)}$, i.e. $\overline{\Gamma^{(j_0)}} = \overline{\Omega^{(i_0)}} \cap \overline{\Omega^{(i_1)}}$. Then, we construct the vertex subspace $\mathcal{W}_{\mathbf{v}^{(i)}}$ as

$$\mathcal{W}_{\mathbf{v}^{(i)}} = \text{span}\{\phi_{\mathbf{v}_2^{(i)};j_1,j_2} \mid j_1 = 0, 1, \dots, 4, j_2 = 0, 1, \dots, 4 - \min(j_1, 2)\},$$

where $\phi_{\mathbf{v}_2^{(i)};j_1,j_2}$ is given as

$$\phi_{\mathbf{v}_2^{(i)};j_1,j_2}(\mathbf{x}) = \begin{cases} \phi_{\Gamma_I^{(j_0)};j_1,j_2}(\mathbf{x}) & \text{if } j_1 = 0, 1, 2, \\ \phi_{\Omega^{(i_0)};j_1+\lfloor \frac{j_2}{2} \rfloor, j_2 \bmod 2}(\mathbf{x}) & \text{if } j_1 = 3, \\ \phi_{\Omega^{(i_1)};j_1-1+\lfloor \frac{j_2}{2} \rfloor, j_2 \bmod 2}(\mathbf{x}) & \text{if } j_1 = 4, \end{cases} \quad (17)$$

with the functions $\phi_{\Omega^{(i_\ell)};j_1,j_2}$ and $\phi_{\Gamma_I^{(j_0)};j_1,j_2}$ as defined in (5) and (7), respectively. The functions $\phi_{\mathbf{v}_2^{(i)};j_1,j_2}$ are C^2 -smooth on $\bar{\Omega}$, since the functions $\phi_{\Gamma_I^{(j_0)};j_1,j_2}$, $j_1 = 0, 1, 2$, $j_2 = 0, \dots, 4 - j_1$, are C^2 -smooth on $\bar{\Omega}$ by construction, and the functions $\phi_{\Omega^{(i_\ell)};j_1,j_2}$, $j_1 = 3, 4$, $j_2 = 0, 1, \dots, 1 - j_1 + 3$, $\ell = 0, 1$, possess vanishing values, gradients and Hessians along all interfaces $\Gamma^{(j)}$, $j \in \mathcal{I}_{\Gamma_I}$

Finally, for the case of a boundary vertex $\mathbf{v}^{(i)}$ of patch valency $\nu_i = 1$, i.e. $i \in \mathcal{I}_{\Xi_1}$, and assuming without loss of generality that the vertex $\mathbf{v}^{(i)}$ is given by $\mathbf{v}^{(i)} = \mathbf{F}^{(i_0)}(\mathbf{0})$, the vertex subspace $\mathcal{W}_{\mathbf{v}^{(i)}}$ is of the form

$$\mathcal{W}_{\mathbf{v}^{(i)}} = \text{span}\{\phi_{\mathbf{v}_1^{(i)};j_1,j_2} \mid j_1, j_2 = 0, 1, \dots, 4, j_1 + j_2 \leq 4\},$$

where $\phi_{\mathbf{v}_1^{(i)};j_1,j_2}$ is defined as

$$\phi_{\mathbf{v}_1^{(i)};j_1,j_2}(\mathbf{x}) = \begin{cases} (N_{j_1,j_2}^{p,r} \circ (\mathbf{F}^{(i_0)})^{-1})(\mathbf{x}) & \text{if } \mathbf{x} \in \overline{\Omega^{(i_0)}}, \\ 0 & \text{otherwise.} \end{cases} \quad (18)$$

The functions $\phi_{\mathbf{v}_1^{(i)};j_1,j_2}$ are trivially C^2 -smooth on $\overline{\Omega}$, since the functions have vanishing values, gradients and Hessians along all interfaces $\overline{\Gamma^{(j)}}$, $j \in \mathcal{I}_{\Gamma_I}$.

One could generate for the case of a boundary vertex $\mathbf{v}^{(i)}$ of patch valency $\nu_i = 2$ or $\nu_i = 1$ a different vertex subspace $\mathcal{W}_{\mathbf{v}^{(i)}}$ as described above by just following also for these cases the strategy explained for a boundary vertex of patch valency $\nu_i \geq 3$. However, we will use in our numerical examples, see Section 4, the construction presented above, since it is simple and does not require the solving of a system of linear equations.

2.4. Basis and dimension of the space \mathcal{W}

Since the space \mathcal{W} is the direct sum (4), a basis of the space \mathcal{W} can be obtained by just constructing bases of the individual subspaces $\mathcal{W}_{\Omega^{(i)}}$, $i \in \mathcal{I}_{\Omega}$, \mathcal{W}_{Γ^i} , $i \in \mathcal{I}_{\Gamma}$, and $\mathcal{W}_{\mathbf{v}^{(i)}}$, $i \in \mathcal{I}_{\Xi}$. As for each collection of functions (5), (6), (7), (12), (16), (17) or (18), spanning one of the subspaces $\mathcal{W}_{\Omega^{(i)}}$, \mathcal{W}_{Γ^i} or $\mathcal{W}_{\mathbf{v}^{(i)}}$, the single functions are linearly independent by construction, the functions form a basis of the corresponding subspace. Moreover, the intersection of any two of the individual subspaces does not have any common function except the zero function. Therefore, the entire collection of all functions, i.e.

$$\begin{aligned} & \phi_{\Omega^{(i)};j_1,j_2}, \quad j_1, j_2 = 3, 4, \dots, n-4, \quad i \in \mathcal{I}_{\Omega}; \\ & \phi_{\Gamma_B^{(i)};j_1,j_2}, \quad j_1 = 0, 1, 2, \quad j_2 = 5 - j_1, \dots, n + j_1 - 6, \quad i \in \mathcal{I}_{\Gamma_B}; \\ & \phi_{\Gamma_I^{(i)};j_1,j_2}, \quad j_1 = 0, 1, 2, \quad j_2 = 5 - j_1, \dots, n_{j_1} + j_1 - 6, \quad i \in \mathcal{I}_{\Gamma_I}; \\ & \phi_{\mathbf{v}_I^{(i)};j_1,j_2}, \quad j_1, j_2 = 0, 1, \dots, 4, \quad j_1 + j_2 \leq 4, \quad i \in \mathcal{I}_{\Xi_I}; \\ & \phi_{\mathbf{v}_3^{(i)};j_1,j_2}, \quad j_1, j_2 = 0, 1, \dots, 4, \quad j_1 + j_2 \leq 4, \quad i \in \mathcal{I}_{\Xi_3}; \\ & \phi_{\mathbf{v}_2^{(i)};j_1,j_2}, \quad j_1 = 0, 1, \dots, 4, \quad j_2 = 0, 1, \dots, 4 - \min(j_1, 2), \quad i \in \mathcal{I}_{\Xi_2}; \end{aligned}$$

and

$$\phi_{\mathbf{v}_1^{(i)};j_1,j_2}, \quad j_1, j_2 = 0, 1, \dots, 4, \quad j_1 + j_2 \leq 4, \quad i \in \mathcal{I}_{\Xi_1};$$

builds a basis of the space \mathcal{W} , cf. [27, Theorem 1].

In addition, the decomposition (4) of the space \mathcal{W} implies that

$$\dim \mathcal{W} = \sum_{i \in \mathcal{I}_\Omega} \dim \mathcal{W}_{\Omega^{(i)}} + \sum_{i \in \mathcal{I}_\Gamma} \dim \mathcal{W}_{\Gamma^{(i)}} + \sum_{i \in \mathcal{I}_\Xi} \dim \mathcal{W}_{\mathbf{v}^{(i)}}.$$

Since the dimensions of the single subspaces $\mathcal{W}_{\Omega^{(i)}}$, $i \in \mathcal{I}_\Omega$, $\mathcal{W}_{\Gamma^{(i)}}$, $i \in \mathcal{I}_\Gamma$, and $\mathcal{W}_{\mathbf{v}^{(i)}}$, $i \in \mathcal{I}_\Xi$, are given by

$$\dim \mathcal{W}_{\Omega^{(i)}} = (n - 6)^2,$$

$$\dim \mathcal{W}_{\Gamma^{(i)}} = \begin{cases} 3(n - 8) & \text{if } i \in \mathcal{I}_{\Gamma_B}, \\ 3(n - 2k - 9) & \text{if } i \in \mathcal{I}_{\Gamma_I}, \end{cases}$$

and

$$\dim \mathcal{W}_{\mathbf{v}^{(i)}} = \begin{cases} 15 & \text{if } i \in \mathcal{I}_{\Xi_I} \cup \mathcal{I}_{\Xi_1} \cup \mathcal{I}_{\Xi_3}, \\ 18 & \text{if } i \in \mathcal{I}_{\Xi_2}, \end{cases}$$

respectively, the dimension of \mathcal{W} is equal to

$$\dim \mathcal{W} = |\mathcal{I}_\Omega|(n-6)^2 + 3|\mathcal{I}_{\Gamma_I}|(n-2k-9) + 3|\mathcal{I}_{\Gamma_B}|(n-8) + 15(|\mathcal{I}_{\Xi_I}| + |\mathcal{I}_{\Xi_1}| + |\mathcal{I}_{\Xi_3}|) + 18|\mathcal{I}_{\Xi_2}|. \quad (19)$$

Therefore, in contrast to [27], the dimension of the C^2 -smooth space \mathcal{W} is independent of the initial geometry.

3. Isogeometric collocation

We will present the idea of using the concept of isogeometric collocation for solving the Poisson's equation on planar multi-patch domains.

3.1. Problem statement and isogeometric formulation

Let $f : \Omega \rightarrow \mathbb{R}$, $f_1 : \partial\Omega \rightarrow \mathbb{R}$. We are interested in finding $u : \bar{\Omega} \rightarrow \mathbb{R}$, $u \in C^2(\bar{\Omega})$, which solves the Poisson's equation

$$\begin{aligned} \Delta u(\mathbf{x}) &= f(\mathbf{x}), & \mathbf{x} \in \Omega, \\ u(\mathbf{x}) &= f_1(\mathbf{x}), & \mathbf{x} \in \partial\Omega. \end{aligned} \quad (20)$$

The idea is to employ isogeometric collocation to compute a C^2 -smooth approximation $u_h \in \mathcal{W}$ of the solution u . This requires the use of global collocation points \mathbf{y}_j , $j \in \mathcal{J}$, which are separated into two distinct sets of collocation points, namely of inner collocation points \mathbf{y}_j^I , $j \in \mathcal{J}_I$, and of boundary collocation points \mathbf{y}_j^B , $j \in \mathcal{J}_B$. Inserting these points into (20), we obtain

$$\begin{aligned} \Delta u(\mathbf{y}_j^I) &= f(\mathbf{y}_j^I), & j \in \mathcal{J}_I, \\ u(\mathbf{y}_j^B) &= f_1(\mathbf{y}_j^B), & j \in \mathcal{J}_B. \end{aligned} \quad (21)$$

To use the isogeometric approach for solving problem (21), we have to express each global collocation point \mathbf{y}_j with respect to local coordinates via

$$\zeta_j^{(\delta(j));I} = \left(\mathbf{F}^{(\delta(j))}\right)^{-1}(\mathbf{y}_j^I), \quad j \in \mathcal{J}_I, \quad \text{and} \quad \zeta_j^{(\delta(j));B} = \left(\mathbf{F}^{(\delta(j))}\right)^{-1}(\mathbf{y}_j^B), \quad j \in \mathcal{J}_B,$$

where

$$\delta : \mathcal{J} \rightarrow \mathcal{I}_\Omega, \quad \delta(j) = \min\{i \in \mathcal{I}_\Omega, \mathbf{y}_j \in \overline{\Omega^{(i)}}\}.$$

Having the local collocation points $\zeta_j^{(\delta(j));I}$ and $\zeta_j^{(\delta(j));B}$, then equations (21) can be transformed into

$$\frac{1}{\left|\det J^{(\delta(j))}(\zeta_j^{(\delta(j));I})\right|} \left(\nabla \circ \left(N^{(\delta(j))}(\boldsymbol{\xi}) \nabla(u \circ \mathbf{F}^{(\delta(j))})(\boldsymbol{\xi}))\right)\right) \Big|_{\boldsymbol{\xi}=\zeta_j^{(\delta(j));I}} = f\left(\mathbf{F}^{(\delta(j))}\left(\zeta_j^{(\delta(j));I}\right)\right), \quad j \in \mathcal{J}_I,$$

$$u\left(\mathbf{F}^{(\delta(j))}\left(\zeta_j^{(\delta(j));B}\right)\right) = f_1\left(\mathbf{F}^{(\delta(j))}\left(\zeta_j^{(\delta(j));B}\right)\right), \quad j \in \mathcal{J}_B,$$

where $J^{(\ell)}$ is the Jacobian of $\mathbf{F}^{(\ell)}$ and

$$N^{(\ell)}(\boldsymbol{\xi}) = \left(J^{(\ell)}(\boldsymbol{\xi})\right)^{-T} \left(J^{(\ell)}(\boldsymbol{\xi})\right)^{-1} \left|\det J^{(\ell)}(\boldsymbol{\xi})\right|.$$

This gives rise to a linear system for the unknown coefficients c_i of the approximation $u_h = \sum_{i \in \mathcal{I}} c_i \phi_i$, where $\mathcal{I} = \{0, 1, \dots, \dim \mathcal{W} - 1\}$, and $\{\phi_i\}_{i \in \mathcal{I}}$ is the basis of \mathcal{W} presented in Section 2.4.

3.2. Selection of collocation points

The choice of the collocation points plays an important role in the stability and convergence behavior of the numerical solution. Below, we will first present the general concept of choosing these points, and will then describe in more detail two particular selections of the collocation points.

3.2.1. The general concept

The idea is to choose for each patch $\overline{\Omega^{(i)}}$, $i \in \mathcal{I}_\Omega$, global collocation points $\mathbf{F}^{(i)}(\zeta_j)$, which are determined by the local collocation points

$$\zeta_j = (\zeta_{j1}, \zeta_{j2}) \in [0, 1]^2, \quad (22)$$

which are again composed of univariate collocation points $\zeta_j \in [0, 1]$. In case that we obtain the same global collocation point for more than one patch, we keep the corresponding point just for the patch $\overline{\Omega^{(i)}}$ with the smallest index i , to avoid repetitions of points. Moreover, we split the resulting points into inner and boundary collocation points, cf. Section 3.1.

In the one-patch case, mainly two different types of (univariate) collocation points have been considered. First, standard collocation points such as Greville abscissae or Demko abscissae are used, see e.g. [2, 30, 36], and possess a convergence behavior with respect³

³Instead of studying the convergence behavior with respect to the L^2 , H^1 and H^2 norm, often equivalently, the L^∞ , $W^{1,\infty}$ and $W^{2,\infty}$ -norm is considered in the literature.

to the L^2 , H^1 and H^2 norm of orders $\mathcal{O}(h^{p-1})$, $\mathcal{O}(h^{p-1})$ and $\mathcal{O}(h^{p-1})$ and of orders $\mathcal{O}(h^p)$, $\mathcal{O}(h^p)$ and $\mathcal{O}(h^{p-1})$ for odd and even spline degree p , respectively. These convergence rates are suboptimal for the L^2 norm and in the case of odd spline degree p also for the H^1 norm in comparison to the Galerkin approach, where the rates are of orders $\mathcal{O}(h^{p+1})$, $\mathcal{O}(h^p)$ and $\mathcal{O}(h^{p-1})$.

The second type of collocation points are the so-called superconvergent points [1, 15, 32], which provide in case of odd spline degree p better convergence rates than the Greville abscissae. In more detail, in case of odd spline degree, the convergence behavior for the approach [15] is of orders $\mathcal{O}(h^p)$, $\mathcal{O}(h^p)$ and $\mathcal{O}(h^{p-1})$ with respect to L^2 , H^1 and H^2 norm, and the convergence rates for the methods [1, 32] are even of optimal orders, i.e. $\mathcal{O}(h^{p+1})$, $\mathcal{O}(h^p)$ and $\mathcal{O}(h^{p-1})$ with respect to L^2 , H^1 and H^2 norm. The basic concept of the superconvergent points is to choose as collocation points those points (or more precisely approximations of those points), which are the roots of the Galerkin residual $D^2(u - u_h)$ of the considered problem. Since the resulting set of superconvergent points is approximately twice as large as the number of degrees of freedom, different strategies have been proposed in [1, 15, 32] to use the superconvergent points as collocation points for solving the collocation problem (21). In [1], the entire set of points is used, which leads to an overdetermined linear system that is solved by means of the least-squares method. In contrast, in [15, 32], particular subsets of superconvergent points are selected to obtain the same number of collocation points as the number of degrees of freedom. While the superconvergent points are selected in [15] in an alternating way, the points are chosen in [32] in a clustered way.

Below, we will extend the use of Greville abscissae and of superconvergent points as collocation points to the case of planar multi-patch domains. One main difference will be that splines of maximal smoothness, i.e. $r = p - 1$, as usually employed in the one-patch case, cannot be used for the multi-patch case. In the latter case, the underlying spline spaces $\mathcal{S}_h^{p,r}$ have to fulfill $2 \leq r \leq p - 3$ with $p \geq 5$ to allow the construction of h -refineable C^2 -smooth spline spaces \mathcal{W} , cf. Section 2.1 and Section 2.3. For the sake of simplicity, we will restrict ourselves to the cases $(p, r) \in \{(5, 2), (6, 2), (6, 3)\}$. In addition, the number of collocation points will be slightly larger than the number of degrees of freedom, cf. Section 3.2.2 and Section 3.2.3. Therefore, the resulting linear system will be overdetermined and will be solved as in [1] by means of the least-squares method. As already observed in [1], we first have to solve those equations in (21) which have been determined by the boundary collocation points, i.e. the second set of equations, and then use the result to solve the remaining system of linear equations.

3.2.2. Greville abscissae

For each patch $\overline{\Omega^{(i)}}$, $i \in \mathcal{I}_\Omega$, the local collocation points ζ_j , $j \in \{0, 1, \dots, n-1\}^2$, from (22) are chosen as the tensor-product Greville points

$$\zeta_j^{p,r} = (\zeta_{j_1}^{p,r}, \zeta_{j_2}^{p,r})$$

with $\zeta_j^{p,r} = \frac{t_{j+1}^{p,r} + \dots + t_{j+p}^{p,r}}{p}$, $j \in \{0, 1, \dots, n-1\}$. The resulting global collocation points $\mathbf{F}^{(i)}(\zeta_j^{p,r})$ for a particular example of a bilinearly parameterized three-patch domain are shown in Fig. 2. As already mentioned in the previous section, the number of (global) collocation

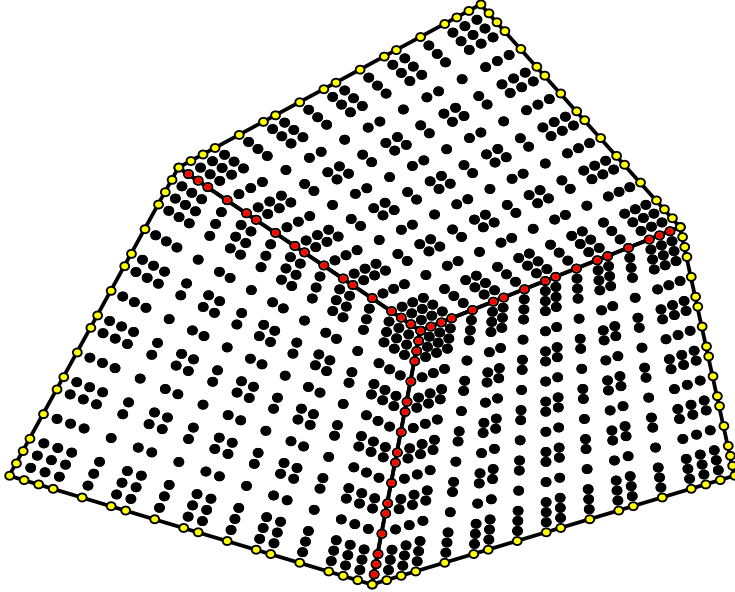


Figure 2: Set of all mapped Greville points $F^{(i)}(\zeta_j^{(5,2)})$ (without repetitions) for a bilinearly parameterized three-patch domain and $k = 4$, where the boundary collocation points and the collocation points on the interfaces are specified in yellow and red, respectively.

points (without repetitions of same points) is slightly larger than the number of basis functions of the C^2 -smooth space \mathcal{W} . But the quotient of the number of collocation points and of the number of basis functions converges to 1 when k grows as the following example will demonstrate.

Example 1. Let $\bar{\Omega}$ be a multi-patch domain with exactly one inner vertex of edge and patch valency ν , see e.g. the three-, five- and six-patch domain in Fig 6 (a)–(c). In addition, let $p = 5$ and $r = 2$, which implies $n = 6 + 3k$. Since $\dim \mathcal{W} = \nu(9k^2 + 21k + 12) + 15$ (compare formula (19)) and the number of collocation points (without repetitions), i.e. $|\mathcal{J}|$, is equal to $\nu n^2 - \nu n + 1 = \nu(9k^2 + 33k + 30) + 1$, we obtain

$$\lim_{k \rightarrow \infty} \frac{|\mathcal{J}|}{\dim \mathcal{W}} = \lim_{k \rightarrow \infty} \frac{\nu(9k^2 + 33k + 30) + 1}{\nu(9k^2 + 21k + 12) + 15} = 1.$$

Note that the same conclusion is not only true for $(p, r) = (6, 2)$ and $(p, r) = (6, 3)$ but also for any multi-patch domain, since the number of collocation points is just slightly larger than the number of basis functions along the edges and in the vicinity of inner vertices and boundary vertices of patch valencies greater or equal to two.

The numerical results in Section 4 will show that we will obtain for the multi-patch case the same convergence behavior as for the one-patch case, namely with respect to the L^2 , H^1 and H^2 norm, convergence rates of orders $\mathcal{O}(h^{p-1})$, $\mathcal{O}(h^{p-1})$ and $\mathcal{O}(h^{p-1})$ and of orders $\mathcal{O}(h^p)$, $\mathcal{O}(h^p)$ and $\mathcal{O}(h^{p-1})$ for odd and even spline degree p , respectively.

3.2.3. Superconvergent points

The superconvergent points (cf. [1, 15, 32]) are defined as the roots of the Galerkin residual $D^2(u - u_h)$ of the considered problem. Estimates of the univariate superconvergent points can be computed by solving a simple 1D Poisson's equation such as

$$u''(x) = f(x), \quad x \in (0, 1), \quad \text{and} \quad u(0) = u(1) = 0, \quad (23)$$

with some particular function f . The superconvergent points have been mainly considered so far just for splines of maximal smoothness, i.e., $r = p - 1$. Since the C^2 -smooth spline spaces \mathcal{W} require underlying spline spaces $\mathcal{S}_h^{p,r}$ with $2 \leq r \leq p - 3$ and $p \geq 5$, cf. Section 2.1 and Section 2.3, we will generate these points for some of these spaces, namely for the cases $(p, r) \in \{(5, 2), (6, 2), (6, 3)\}$. To first estimate the superconvergent points, we just follow the approach presented in [15] based on a particular 1D Poisson's problem (23). Further studying the asymptotic behavior of the resulting estimates of the superconvergent points for the different levels of refinement, we obtain that the superconvergent points on each knot span with respect to the reference interval $[-1, 1]$ are given as the roots of the polynomial $15x^4 - 12x^2 + 1$ for $p = 5$ and $r = 2$ and as the roots of the polynomial $99x^5 - 130x^3 + 31x$ for $p = 6$ and $r = 2, 3$. The roots of these polynomials, and hence the locations of the superconvergent points on each knot span with respect to the reference interval $[-1, 1]$ are presented in Table 1. All superconvergent points for $(p, r) = (5, 2)$ and $(p, r) \in \{(6, 2), (6, 3)\}$ are shown in Fig. 3 and 4, respectively. In case of $(p, r) \in$

(p, r)	Superconvergent points
(5,2)	$\pm\sqrt{\frac{1}{15}(6 + \sqrt{21})}, \quad \pm\sqrt{\frac{1}{15}(6 - \sqrt{21})}$
(6,2)	$0, \quad \pm 1, \quad \pm\sqrt{\frac{31}{99}}$
(6,3)	$0, \quad \pm 1, \quad \pm\sqrt{\frac{31}{99}}$

Table 1: Locations of the superconvergent points on each knot span w.r.t. the reference interval $[-1, 1]$ for the cases $(p, r) \in \{(5, 2), (6, 2), (6, 3)\}$.

$\{(6, 2), (6, 3)\}$, the knots of the underlying spline spaces $\mathcal{S}_h^{p,r}$ are superconvergent points, and therefore, we count these points in case of inner knots just once for two neighboring segments. In case of $(p, r) = (5, 2)$, since the boundary points of the whole domain are not contained in the set of all superconvergent points, they have to be added to the set, see Fig. 3, to be able to impose Dirichlet boundary conditions.

The differences $\Delta_{(p,r)}$ between the number of all superconvergent points and the dimension of the underlying spline space $\mathcal{S}_h^{p,r}$ (i.e. $\dim \mathcal{S}_h^{p,r} = p + 1 + k(p - r)$) are given by

$$\begin{aligned} \Delta_{(5,2)} &= 4(k + 1) + 2 - (6 + 3k) = k, \\ \Delta_{(6,2)} &= 4(k + 1) + 1 - (7 + 4k) = -2, \\ \Delta_{(6,3)} &= 4(k + 1) + 1 - (7 + 3k) = k - 2. \end{aligned}$$

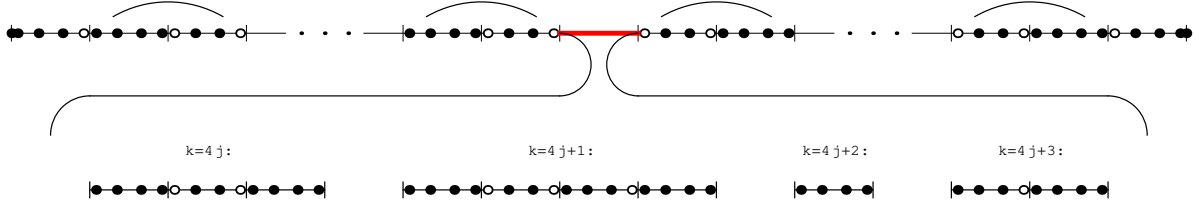


Figure 3: All superconvergent points (black and white points) and clustered superconvergent points (only black points) for the case $(p, r) = (5, 2)$. The center part (in red) is given by the second row depending on the number k of different inner knots.

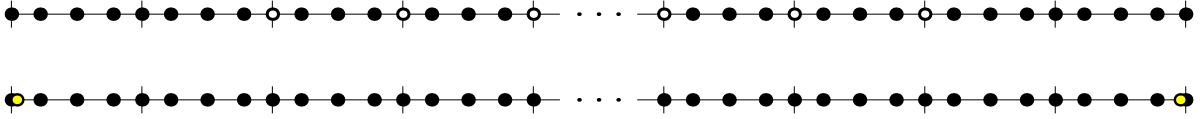


Figure 4: First row: All superconvergent points (black and white points) and clustered superconvergent points (only black points) for $(p, r) = (6, 3)$. Second row: All superconvergent points (black and yellow points), which coincide with the clustered superconvergent points, for the case $(p, r) = (6, 2)$, where the yellow points specify the two added Greville abscissae.

The idea is to select from the superconvergent points in a clustered way a subset of collocation points such that the number of collocation points is equal to the number of basis functions of $\mathcal{S}_h^{p,r}$, and such that the selection of points does not ruin the convergence properties as in [32] for the case of splines of maximal smoothness. While in the case of $(p, r) = (6, 2)$, we have even to add two points to the set of superconvergent points, in the cases $(p, r) = (5, 2)$ and $(p, r) = (6, 3)$ we have to omit k and $k - 2$ points, respectively. We will call the resulting sets of collocation points clustered superconvergent points similarly to [32].

Let us first consider the case $(p, r) = (6, 2)$. We choose as additional points for the set of superconvergent points just the second and the second last Greville abscissa. This strategy has been already used for selecting additional points close to the boundary for Dirichlet boundary problems in case of splines of maximal smoothness, cf. [15, 32]. Note that for $(p, r) = (6, 2)$ the set of all superconvergent points coincides with the set of clustered superconvergent points.

Recall that for the cases $(p, r) = (5, 2)$ and $(p, r) = (6, 3)$ we have to omit k and $k - 2$ points, respectively. We denote by S_k the indices of the points which will be omitted. Furthermore, we can assume $k \geq 2$. For $(p, r) = (5, 2)$, we choose depending on the number k of different inner knots the set S_k as

$$S_k = \tilde{S}_k \cup \begin{cases} \{2k + 1, 2k + 4\}, & k = 4j, \\ \{2k - 1, 2k + 2, 2k + 6\}, & k = 4j + 1, \\ \{\}, & k = 4j + 2, \\ \{2k + 2\}, & k = 4j + 3, \end{cases}$$

with

$$\tilde{S}_k = \{4, 4k + 1\} \cup \bigcup_{i=0}^{\lfloor \frac{k-6}{4} \rfloor} (\{9 + 8i, 12 + 8i\} \cup \{4k + 5 - (9 + 8i), 4k + 5 - (12 + 8i)\}).$$

In case of $(p, r) = (6, 3)$, we omit all inner knots except the first and the last one, which leads to

$$S_k = \{9 + 4i, i = 0, 1, \dots, k - 3\}.$$

All superconvergent points as well as the clustered superconvergent points are shown in Fig. 3 and 4 for the cases $(p, r) = (5, 2)$ and $(p, r) \in \{(6, 2), (6, 3)\}$, respectively. The following example will demonstrate that these points possess for the one-patch case the same convergence behavior with respect to the L^2 , H^1 and H^2 norm as the sets of all superconvergent points and of the clustered superconvergent points in the case of splines of maximal smoothness. Moreover, it will be shown that also for the case of Greville abscissae we get the same convergence rates for the splines of maximal smoothness and for the splines with a reduced regularity.

Example 2. We perform isogeometric collocation on the one-patch domain in Fig. 5 (first row), which is just the bilinearly parameterized unit square $[0, 1]^2$, and compare the convergence behavior under mesh-refinement for different spline spaces and different sets of collocation points. We use underlying spline spaces $\mathcal{S}_h^{p,r}([0, 1]^2)$ with $p = 5, 6$ and $2 \leq r \leq p - 3$ with mesh sizes $h = \frac{1}{5}, \frac{1}{10}, \frac{1}{20}, \frac{1}{40}$ for $(p, r) = (5, 2)$ and $h = \frac{1}{4}, \frac{1}{8}, \frac{1}{16}, \frac{1}{32}$ for $p = 6$ and $r = 2, 3$. Fig. 5 shows the resulting relative L^2 , H^1 and H^2 errors for the exact solution

$$u(x_1, x_2) = \cos(4x_1 - 2) \sin\left(4x_2 - \frac{2}{3}\right),$$

(see first row), by using the Greville points (second row), all superconvergent points (third row) and the clustered superconvergent points (fourth row) as collocation points. We get as in the case of splines of maximal regularity, see [1, 32], the same rates of convergence depending on the used spline degree p . That is for $p = 5$ in case of Greville points the same rates of order $\mathcal{O}(h^4)$ in the L^2 , H^1 and H^2 norm, and in case of all or clustered superconvergent points the optimal rates of orders $\mathcal{O}(h^6)$, $\mathcal{O}(h^5)$ and $\mathcal{O}(h^4)$ in the L^2 , H^1 and H^2 -norm, respectively. For $p = 6$ we have the same rates independent of one of the three sets of collocation points, that is $\mathcal{O}(h^6)$, $\mathcal{O}(h^6)$ and $\mathcal{O}(h^5)$ in the L^2 , H^1 and H^2 norm, respectively.

In the case of multi-patch domains, see Section 4, the convergence rates for the sets of superconvergent points will be the same as in the one-patch case, except for one particular case, namely for $(p, r) = (5, 2)$ with respect to the L^2 norm, where the rate will be just of order $\mathcal{O}(h^p)$ instead of $\mathcal{O}(h^{p+1})$. In the numerical examples in Section 4, for the sake of brevity, we will restrict ourselves just to the case of clustered superconvergent points, since experiments using all superconvergent points have led to the same convergence rates, and the number of clustered superconvergent points is dramatically smaller than the number

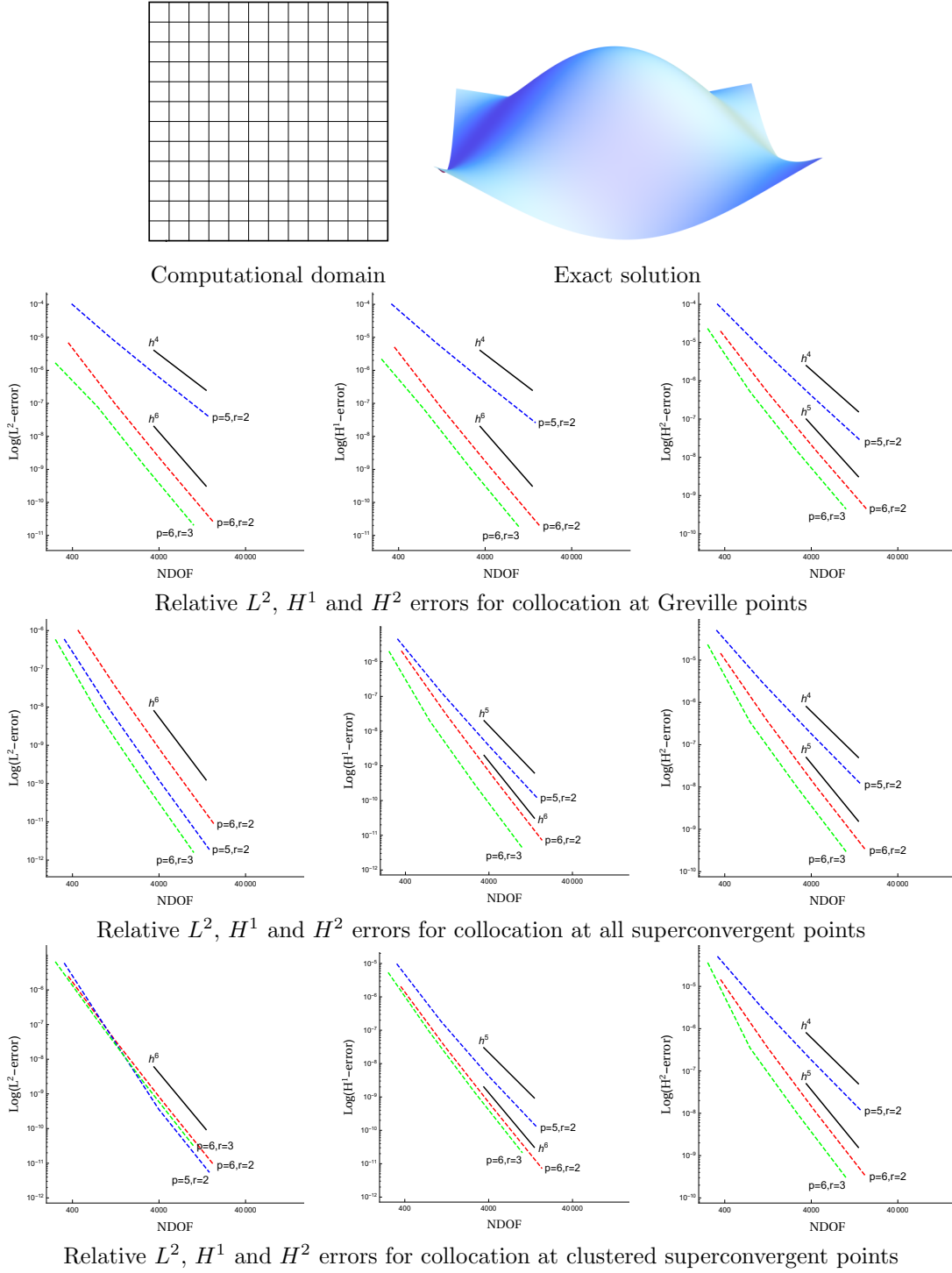


Figure 5: Isogeometric collocation on the bilinearly parameterized unit-square using different sets of collocation points, cf. Example. 2.

of all superconvergent points for the cases $(p, r) = (5, 2)$ and $(p, r) = (6, 3)$. However, in the case of multi-patch domains, also for the clustered superconvergent points the number of points is larger than the number of degrees of freedom. More precisely, the number of clustered superconvergent points is equal to the number of Greville abscissae, and therefore again, the quotient of the number of collocation points and of the number of degrees of freedom converges to one when the number k of different inner knots grows. For solving the resulting overdetermined linear system, we use as for the Greville abscissae the least-squares method.

4. Numerical examples

We will perform isogeometric collocation on several multi-patch domains by using the Greville points and the clustered superconvergent points as collocation points (cf. Section 3.2.2 and Section 3.2.3), and will study the convergence under mesh refinement. Since the considered sets of collocation points will lead to an overdetermined system of linear equations, we will use the least-squares approach to solve the system, see Section 3.2. Below, we will denote the C^2 -smooth space \mathcal{W} for a specific mesh size h by \mathcal{W}_h .

Example 3. We consider the four bilinearly parameterized multi-patch domains (a)-(d) shown in Fig. 6 (first row). For all domains we generate a sequence of C^2 -smooth spaces \mathcal{W}_h with mesh sizes $h = \frac{1}{5}, \frac{1}{10}, \frac{1}{20}, \frac{1}{40}$ for $p = 5$ and $r = 2$ and with mesh sizes $h = \frac{1}{4}, \frac{1}{8}, \frac{1}{16}, \frac{1}{32}$ for $p = 6$ and $r = 2, 3$. The generated C^2 -smooth spaces are then used to perform isogeometric collocation on the different multi-patch domains for a right side function f obtained from the exact solutions u visualized in Fig. 6 (a)-(d), which are given for the single domains (a)-(d) by

$$\begin{aligned} u_a(x_1, x_2) &= -4 \cos\left(\frac{2x_1}{3}\right) \sin\left(\frac{2x_2}{3}\right), \\ u_b(x_1, x_2) &= -4 \cos\left(\frac{x_1}{2}\right) \sin\left(\frac{x_2 - 2}{2}\right), \\ u_c(x_1, x_2) &= -4 \cos\left(\frac{x_1 + 3}{2}\right) \sin\left(\frac{x_2 - 1}{2}\right), \end{aligned}$$

and

$$u_d(x_1, x_2) = -4 \cos\left(\frac{x_1}{3}\right) \sin\left(\frac{x_2}{3}\right),$$

respectively. The resulting relative L^2 , H^1 and H^2 errors by using Greville points and clustered superconvergent points are shown in Fig. 7 and 8, respectively. In case of Greville points the estimated convergence rates are the same as for the one-patch instance in Example 2, that is for $p = 5$ the same rates of order $\mathcal{O}(h^4)$ in the L^2 , H^1 and H^2 norm, and for $p = 6$ the rates of orders $\mathcal{O}(h^6)$, $\mathcal{O}(h^6)$ and $\mathcal{O}(h^5)$ in the L^2 , H^1 and H^2 norm, respectively. In case of clustered superconvergent points, we observe for both spline degrees $p = 5, 6$ convergence rates of orders $\mathcal{O}(h^p)$, $\mathcal{O}(h^p)$ and $\mathcal{O}(h^{p-1})$ in the L^2 , H^1 and H^2 norm, respectively, which means for $p = 5$ a reduction of the order by 1 with respect

to the L^2 norm compared to the one-patch instance in Example 2. Note that using all superconvergent points would lead to the same reduced rate for $p = 5$ as employing clustered superconvergent points, and therefore will not be shown for the sake of brevity.

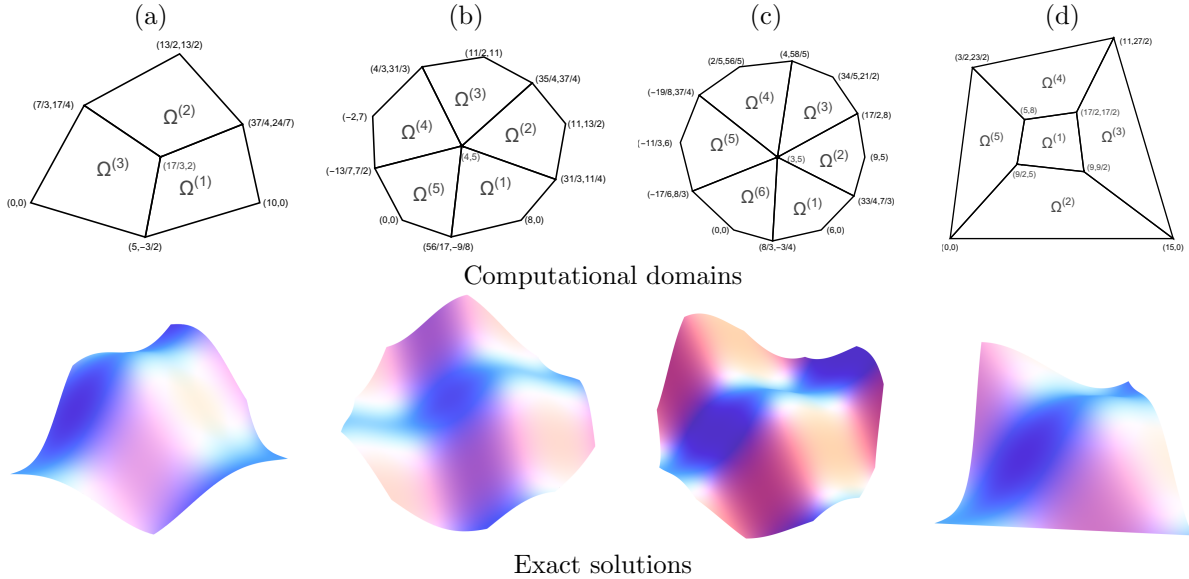


Figure 6: Computational domains and exact solutions for performing isogeometric collocation in Example 3 (see also Fig. 7 and 8).

Example 4. We consider the bicubic three-patch spline geometry taken from [27, Example 4], which is also visualized in Fig. 9 (first row). Since the geometry is parameterized in such a way that it is bilinear close to the patch interfaces (cf. Appendix A for the spline control points of the geometry), our approach can be also applied to this more general multi-patch domain. We perform isogeometric collocation on this domain for the right side function f obtained from the exact solution

$$u(x_1, x_2) = -4 \cos\left(\frac{2x_1}{3}\right) \sin\left(\frac{2x_2}{3}\right),$$

see Fig. 6 (first row), by employing C^2 -smooth spaces \mathcal{W}_h with mesh sizes $h = \frac{1}{4}, \frac{1}{8}, \frac{1}{16}, \frac{1}{32}$ for $p = 5, 6$ and $r = 2$. Again, we compare the resulting relative L^2 , H^1 and H^2 errors by using Greville points, see Fig. 9 (second row), and clustered superconvergent points, see Fig. 9 (third row), for collocation, and observe the same rates of convergence as in Example 3.

5. Conclusion

We have presented a method for computing a globally C^2 -smooth approximation of the solution of the Poisson's equation over planar bilinearly parameterized multi-patch domains. Our technique is based on the concept of isogeometric collocation and on the use

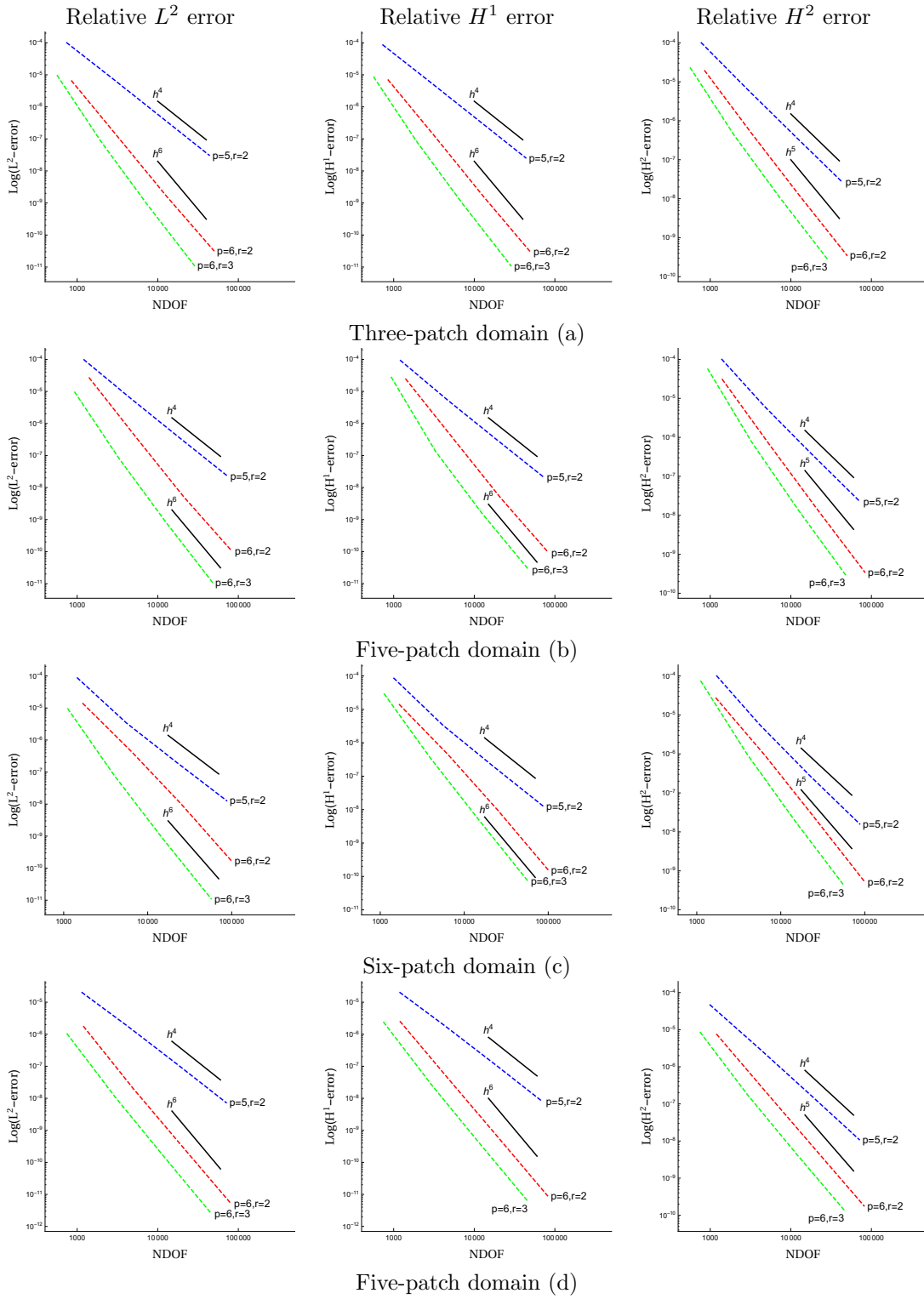


Figure 7: Error plots w.r.t. the number of degrees of freedom (NDOF) of performing isogeometric collocation on the different multi-patch domains given in Fig. 6 (first row) for right side functions obtained by the exact solutions shown in Fig 6 (second row) using the Greville points as collocation points.

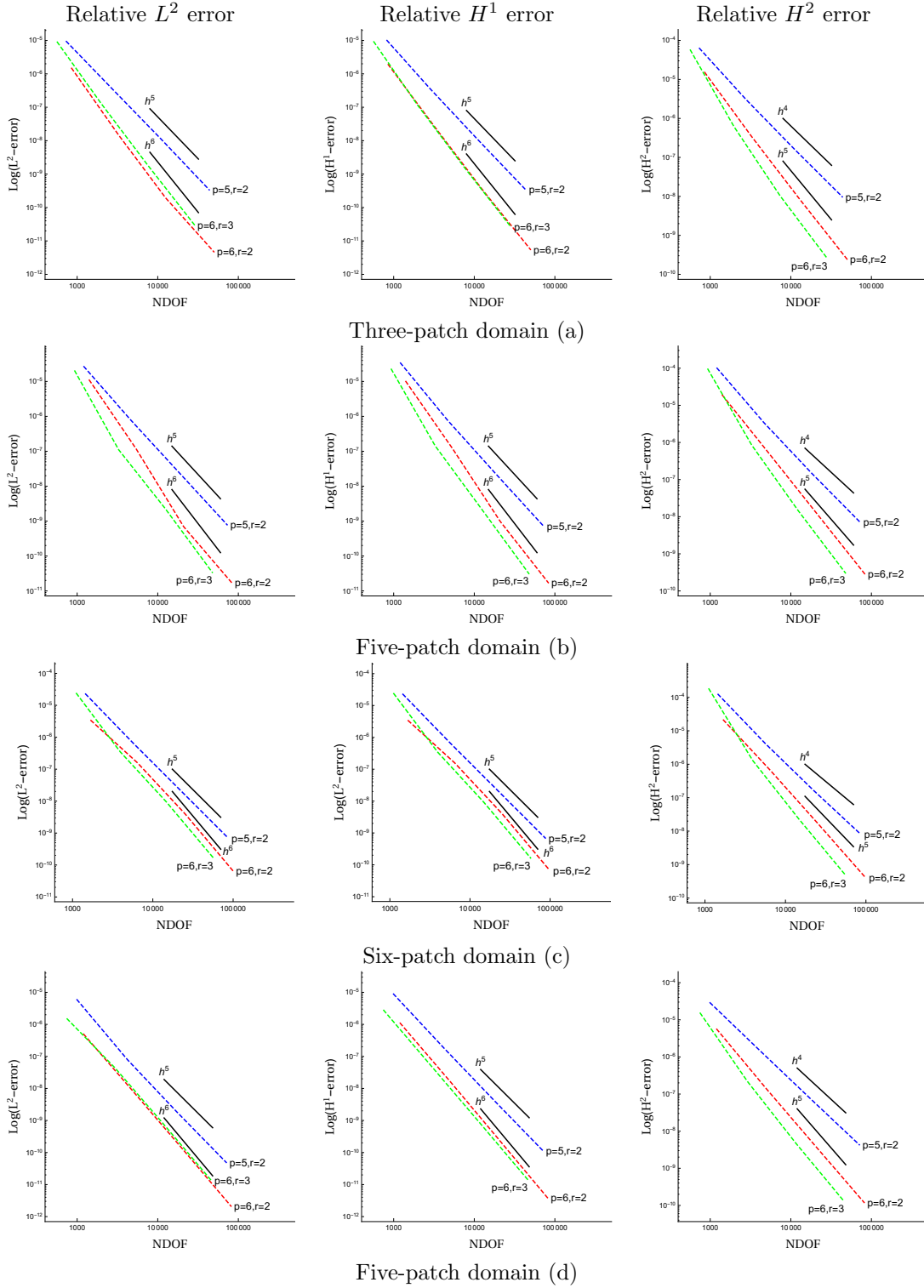
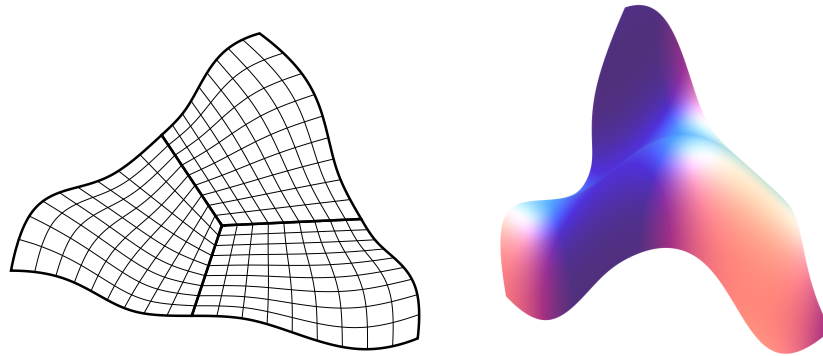
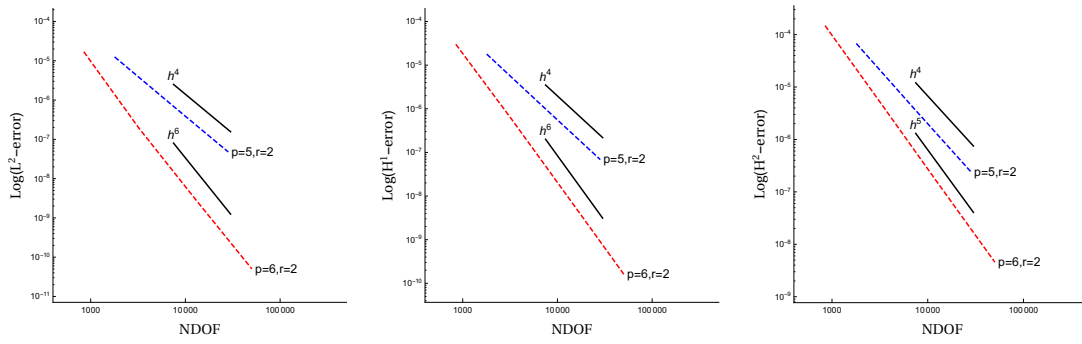


Figure 8: Error plots w.r.t. the number of degrees of freedom (NDOF) of performing isogeometric collocation on the different multi-patch domains given in Fig. 6 (first row) for right side functions obtained by the exact solutions shown in Fig 6 (second row) using the clustered superconvergent points as collocation points.

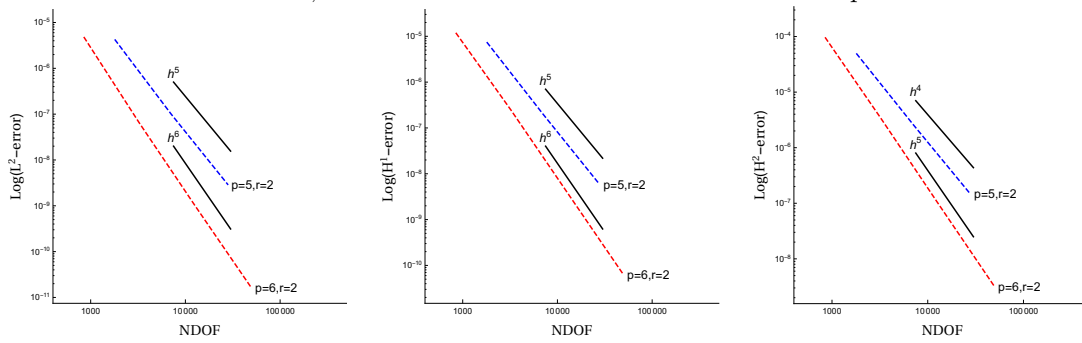


Computational domain

Exact solution



Relative L^2 , H^1 and H^2 errors for collocation at Greville points



Relative L^2 , H^1 and H^2 errors for collocation at clustered superconvergent points

Figure 9: Isogeometric collocation on a bicubic three-patch spline geometry using different sets of collocation points, cf. Example. 4.

of a globally C^2 -smooth isogeometric spline space as discretization space. The constructed C^2 -smooth space is a particular subspace of the space of all globally C^2 -smooth isogeometric spline functions on the considered multi-patch domain, and can be generated as the direct sum of simpler spaces corresponding to the individual patches, edges and vertices of the multi-patch domain. Moreover, the C^2 -smooth space possesses a dimension independent of the initial geometry, and the construction of a basis with locally supported functions is simple and works uniformly for all possible multi-patch configurations.

Two different approaches for the choice of the collocation points have been proposed, where both strategies can be seen as the extension of successfully tested techniques in the one-patch case. On the one hand, we employ the tensor-product Greville points, and on the other hand, we generalize the concept of superconvergent points (cf. [1, 15, 32]) to the case of planar multi-patch domains. While in the one-patch case splines of maximal smoothness, i.e. $r = p - 1$, are normally used, the C^2 -smooth multi-patch spline spaces require underlying spline spaces $\mathcal{S}_h^{p,r}$ of regularity $2 \leq r \leq p - 3$. For the sake of simplicity, we have restricted ourselves to the cases $(p, r) \in \{(5, 2), (6, 2), (6, 3)\}$.

For both choices of the collocation points, the numerical results have shown the same convergence behavior with respect to L^2 , H^1 and H^2 norm as in the one-patch case except in one particular case for the superconvergent points. Namely, in case of $(p, r) = (5, 2)$, the convergence rates with respect to L^2 norm seems to be always reduced by one order, that is $\mathcal{O}(h^5)$ instead of the possible order of $\mathcal{O}(h^6)$ in the one-patch case. However, already this slightly reduced convergence behavior in the L^2 norm is better as the one for the case of Greville points, where the obtained convergence rates are just of order $\mathcal{O}(h^4)$ with respect to the L^2 norm.

So far, our isogeometric collocation method is directly applicable only to elliptic PDEs of second order with Dirichlet boundary conditions. To impose also Neumann boundary conditions, further investigations amongst others in connection with the solving of the overdetermined linear system with respect to the fulfillment of the boundary conditions are needed, cf. [1, Remark 2.3.2]. Starting point of these studies could be e.g. the publications [11, 19, 37], where different strategies are described to deal also with Neumann boundary conditions.

The paper leaves several further open issues, which are worth to study. Since the number of collocation points is slightly larger than the dimension of the C^2 -smooth discretization space, the finding of a set of collocation points with the same cardinality as the dimension of the space is of interest to avoid the necessity of the least-squares method for solving the resulting linear system. Clearly, collocation points which lead to optimal convergence rates are of interest, too. However, this is also still an open problem for even spline degree in the one-patch case. A further possible topic could be the extension of our approach to more general multi-patch domains such as bilinear-like parameterizations, cf. [26], or to multi-patch structured shells and multi-patch volumes.

Acknowledgment. The authors wish to thank the anonymous reviewers for their comments that helped to improve the paper. V. Vitrih was partially supported by the Slovenian Research Agency (research program P1-0404 and research projects J1-9186, J1-1715). This support is gratefully acknowledged.

Appendix A. Spline control points of the geometry from Example 4

The spline geometry from Fig. 9 (first row), which was taken from [27, Example 4] and which is also used in Example 4 in this paper, consists of three geometry mappings $\mathbf{F}^{(i)} \in \mathcal{S}_h^{\mathbf{p},r}([0, 1]^2) \times \mathcal{S}_h^{\mathbf{p},r}([0, 1]^2)$, $i = 1, 2, 3$, with $\mathbf{p} = (3, 3)$, $r = (2, 2)$ and $h = 1/4$. Therefore, each geometry mapping $\mathbf{F}^{(i)}$, $i = 1, 2, 3$, possesses a spline parameterization of the form

$$\mathbf{F}^{(i)}(\xi_1, \xi_2) = \sum_{j_1=0}^6 \sum_{j_2=0}^6 \mathbf{c}_{j_1, j_2}^{(i)} N_{j_1, j_2}^{\mathbf{p}, r}(\xi_1, \xi_2),$$

where the single control points $\mathbf{c}_{j_1, j_2}^{(i)}$ are given in Table A.2.

$\mathbf{c}_{j_1, j_2}^{(1)}$						
$(\frac{17}{3}, 2)$	$(\frac{853}{144}, \frac{169}{84})$	$(\frac{103}{16}, \frac{57}{28})$	$(\frac{173}{24}, \frac{29}{14})$	$(\frac{383}{48}, \frac{59}{28})$	$(\frac{1223}{144}, \frac{179}{84})$	$(\frac{35}{4}, \frac{15}{7})$
$(\frac{101}{18}, \frac{11}{6})$	$(\frac{10163}{1728}, \frac{1859}{1008})$	$(\frac{411}{64}, \frac{209}{112})$	$(\frac{2083}{288}, \frac{319}{168})$	$(\frac{4633}{576}, \frac{649}{336})$	$(\frac{14833}{1728}, \frac{1969}{1008})$	$(\frac{425}{48}, \frac{55}{28})$
$(\frac{11}{2}, \frac{3}{2})$	$(\frac{371}{64}, \frac{169}{112})$	$(\frac{409}{64}, \frac{171}{112})$	$(\frac{233}{32}, \frac{87}{56})$	$(\frac{523}{64}, \frac{177}{112})$	$(\frac{561}{64}, \frac{179}{112})$	$(\frac{145}{16}, \frac{45}{28})$
$(\frac{16}{3}, 1)$	$(\frac{1633}{288}, \frac{169}{168})$	$(\frac{203}{32}, \frac{57}{56})$	$(\frac{37}{5}, \frac{99}{100})$	$(\frac{849}{100}, \frac{103}{100})$	$(\frac{923}{100}, \frac{57}{50})$	$(\frac{48}{5}, \frac{121}{100})$
$(\frac{31}{6}, \frac{1}{2})$	$(\frac{3193}{576}, \frac{169}{336})$	$(\frac{403}{64}, \frac{57}{112})$	$(\frac{749}{100}, \frac{8}{25})$	$(\frac{873}{100}, \frac{29}{100})$	$(\frac{961}{100}, \frac{27}{50})$	$(\frac{251}{25}, \frac{13}{20})$
$(\frac{91}{18}, \frac{1}{6})$	$(\frac{9433}{1728}, \frac{169}{1008})$	$(\frac{401}{64}, \frac{19}{112})$	$(\frac{15}{2}, -\frac{21}{100})$	$(\frac{437}{50}, -\frac{12}{25})$	$(\frac{961}{100}, -\frac{6}{25})$	$(\frac{201}{20}, -\frac{1}{14})$
$(5, 0)$	$(\frac{65}{12}, 0)$	$(\frac{25}{4}, 0)$	$(\frac{15}{2}, -\frac{12}{25})$	$(\frac{35}{4}, -\frac{21}{25})$	$(\frac{115}{12}, -\frac{2}{3})$	$(10, -\frac{1}{2})$
$\mathbf{c}_{j_1, j_2}^{(2)}$						
$(\frac{17}{3}, 2)$	$(\frac{50}{9}, \frac{13}{6})$	$(\frac{16}{3}, \frac{5}{2})$	$(5, 3)$	$(\frac{14}{3}, \frac{7}{2})$	$(\frac{40}{9}, \frac{23}{6})$	$(\frac{13}{3}, 4)$
$(\frac{853}{144}, \frac{169}{84})$	$(\frac{10033}{1728}, \frac{2209}{1008})$	$(\frac{3209}{576}, \frac{857}{336})$	$(\frac{167}{32}, \frac{173}{56})$	$(\frac{2803}{576}, \frac{1219}{336})$	$(\frac{8003}{1728}, \frac{4019}{1008})$	$(\frac{325}{72}, \frac{25}{6})$
$(\frac{103}{16}, \frac{57}{28})$	$(\frac{1211}{192}, \frac{251}{112})$	$(\frac{387}{64}, \frac{297}{112})$	$(\frac{181}{32}, \frac{183}{56})$	$(\frac{337}{64}, \frac{435}{112})$	$(\frac{961}{192}, \frac{481}{112})$	$(\frac{39}{8}, \frac{9}{2})$
$(\frac{173}{24}, \frac{29}{14})$	$(\frac{2033}{288}, \frac{389}{168})$	$(\frac{649}{96}, \frac{157}{56})$	$(\frac{127}{20}, \frac{359}{100})$	$(\frac{587}{100}, \frac{441}{100})$	$(\frac{109}{20}, \frac{99}{20})$	$(\frac{523}{100}, \frac{523}{100})$
$(\frac{383}{48}, \frac{59}{28})$	$(\frac{4499}{576}, \frac{803}{336})$	$(\frac{1435}{192}, \frac{331}{112})$	$(\frac{178}{25}, \frac{391}{100})$	$(\frac{661}{100}, \frac{49}{10})$	$(\frac{597}{100}, \frac{279}{50})$	$(\frac{142}{25}, \frac{591}{100})$
$(\frac{1223}{144}, \frac{179}{84})$	$(\frac{14363}{1728}, \frac{2459}{1008})$	$(\frac{4579}{576}, \frac{1027}{336})$	$(\frac{769}{100}, \frac{409}{100})$	$(\frac{73}{10}, \frac{257}{50})$	$(\frac{33}{5}, \frac{583}{100})$	$(\frac{31}{5}, \frac{37}{6})$
$(\frac{35}{4}, \frac{15}{7})$	$(\frac{137}{16}, \frac{69}{28})$	$(\frac{131}{16}, \frac{87}{28})$	$(\frac{799}{100}, \frac{209}{50})$	$(\frac{763}{100}, \frac{263}{50})$	$(\frac{111}{16}, \frac{83}{14})$	$(\frac{13}{2}, \frac{25}{4})$
$\mathbf{c}_{j_1, j_2}^{(3)}$						
$(\frac{17}{3}, 2)$	$(\frac{101}{18}, \frac{11}{6})$	$(\frac{11}{2}, \frac{3}{2})$	$(\frac{16}{3}, 1)$	$(\frac{31}{6}, \frac{1}{2})$	$(\frac{91}{18}, \frac{1}{6})$	$(5, 0)$
$(\frac{50}{9}, \frac{13}{6})$	$(\frac{2365}{432}, \frac{143}{72})$	$(\frac{85}{16}, \frac{13}{8})$	$(\frac{365}{72}, \frac{13}{12})$	$(\frac{695}{144}, \frac{13}{24})$	$(\frac{2015}{432}, \frac{13}{72})$	$(\frac{55}{12}, 0)$
$(\frac{16}{3}, \frac{5}{2})$	$(\frac{749}{144}, \frac{55}{24})$	$(\frac{79}{16}, \frac{15}{8})$	$(\frac{109}{24}, \frac{5}{4})$	$(\frac{199}{48}, \frac{5}{8})$	$(\frac{559}{144}, \frac{5}{24})$	$(\frac{15}{4}, 0)$
$(5, 3)$	$(\frac{115}{24}, \frac{11}{4})$	$(\frac{35}{8}, \frac{9}{4})$	$(\frac{19}{5}, \frac{43}{25})$	$(\frac{83}{25}, \frac{117}{100})$	$(\frac{153}{50}, \frac{7}{10})$	$(\frac{59}{20}, \frac{9}{20})$
$(\frac{14}{3}, \frac{7}{2})$	$(\frac{631}{144}, \frac{77}{24})$	$(\frac{61}{16}, \frac{21}{8})$	$(\frac{61}{20}, \frac{227}{100})$	$(\frac{123}{50}, \frac{181}{100})$	$(\frac{113}{50}, \frac{6}{5})$	$(\frac{43}{20}, \frac{9}{10})$
$(\frac{40}{9}, \frac{23}{6})$	$(\frac{1775}{432}, \frac{253}{72})$	$(\frac{55}{16}, \frac{23}{8})$	$(\frac{251}{100}, \frac{263}{100})$	$(\frac{7}{4}, \frac{113}{50})$	$(\frac{151}{100}, \frac{149}{100})$	$(\frac{17}{12}, 1)$
$(\frac{13}{3}, 4)$	$(\frac{143}{36}, \frac{11}{3})$	$(\frac{13}{4}, 3)$	$(\frac{56}{25}, \frac{141}{50})$	$(\frac{141}{100}, \frac{247}{100})$	$(\frac{10}{9}, \frac{19}{12})$	$(1, 1)$

Table A.2: Control points $\mathbf{c}_{j_1, j_2}^{(i)}$, $i = 1, 2, 3$, of the bicubic three-patch spline geometry shown in Fig. 9 (first row).

References

- [1] C. Anitescu, Y. Jia, Y. J. Zhang, and T. Rabczuk. An isogeometric collocation method using superconvergent points. *Comput. Methods Appl. Mech. Engrg.*, 284:1073–1097, 2015.
- [2] F. Auricchio, L. Beirão da Veiga, T. J. R. Hughes, A. Reali, and G. Sangalli. Isogeometric collocation methods. *Math. Models Methods Appl. Sci.*, 20(11):2075–2107, 2010.
- [3] F. Auricchio, L. Beirão da Veiga, T.J.R. Hughes, A. Reali, and G. Sangalli. Isogeometric collocation for elastostatics and explicit dynamics. *Comput. Methods Appl. Mech. Engrg.*, 249–252:2 – 14, 2012.
- [4] L. Beirão da Veiga, A. Buffa, G. Sangalli, and R. Vázquez. Mathematical analysis of variational isogeometric methods. *Acta Numerica*, 23:157–287, 5 2014.
- [5] L. Beirão da Veiga, C. Lovadina, and A. Reali. Avoiding shear locking for the Timoshenko beam problem via isogeometric collocation methods. *Comput. Methods Appl. Mech. Engrg.*, 241–244:38 – 51, 2012.
- [6] M. Bercovier and T. Matskewich. *Smooth Bézier Surfaces over Unstructured Quadrilateral Meshes*. Lecture Notes of the Unione Matematica Italiana, Springer, 2017.
- [7] A. Blidia, B. Mourrain, and N. Villamizar. G^1 -smooth splines on quad meshes with 4-split macro-patch elements. *Comput. Aided Geom. Des.*, 52-53:106 – 125, 2017.
- [8] C.L. Chan, C. Anitescu, and T. Rabczuk. Isogeometric analysis with strong multipatch C^1 -coupling. *Comput. Aided Geom. Design*, 62:294–310, 2018.
- [9] A. Collin, G. Sangalli, and T. Takacs. Analysis-suitable G^1 multi-patch parametrizations for C^1 isogeometric spaces. *Comput. Aided Geom. Des.*, 47:93 – 113, 2016.
- [10] J. A. Cottrell, T. J. R. Hughes, and Y. Bazilevs. *Isogeometric Analysis: Toward Integration of CAD and FEA*. John Wiley & Sons, Chichester, England, 2009.
- [11] L. De Lorenzis, J. A. Evans, T. J. R Hughes, and A. Reali. Isogeometric collocation: Neumann boundary conditions and contact. *Comput. Methods Appl. Mech. Engrg.*, 284:21 – 54, 2015.
- [12] J. Deng, F. Chen, X. Xin Li, C. Hu, W. Tong, Z. Yang, and Y. Feng. Polynomial splines over hierarchical T-meshes. *Graphical Models*, 70(4):76–86, 2008.
- [13] J. A. Evans, R. R. Hiemstra, T. J. R. Hughes, and A. Reali. Explicit higher-order accurate isogeometric collocation methods for structural dynamics. *Comput. Methods Appl. Mech. Engrg.*, 338:208–240, 2018.

- [14] F. Fahrendorf, L. De Lorenzis, and H. Gomez. Reduced integration at superconvergent points in isogeometric analysis. *Comput. Methods Appl. Mech. Engrg.*, 328:390–410, 2018.
- [15] H. Gomez and L. De Lorenzis. The variational collocation method. *Comput. Methods Appl. Mech. Engrg.*, 309:152–181, 2016.
- [16] D. Groisser and J. Peters. Matched G^k -constructions always yield C^k -continuous isogeometric elements. *Comput. Aided Geom. Des.*, 34:67 – 72, 2015.
- [17] J. Hoschek and D. Lasser. *Fundamentals of computer aided geometric design*. A K Peters Ltd., Wellesley, MA, 1993.
- [18] T. J. R. Hughes, J. A. Cottrell, and Y. Bazilevs. Isogeometric analysis: CAD, finite elements, NURBS, exact geometry and mesh refinement. *Comput. Methods Appl. Mech. Engrg.*, 194(39-41):4135–4195, 2005.
- [19] Y. Jia, C. Anitescu, Y. J. Zhang, and T. Rabczuk. An adaptive isogeometric analysis collocation method with a recovery-based error estimator. *Comput. Methods Appl. Mech. Engrg.*, 345:52–74, 2019.
- [20] M. Kapl, F. Buchegger, M. Bercovier, and B. Jüttler. Isogeometric analysis with geometrically continuous functions on planar multi-patch geometries. *Comput. Methods Appl. Mech. Engrg.*, 316:209 – 234, 2017.
- [21] M. Kapl, G. Sangalli, and T. Takacs. Dimension and basis construction for analysis-suitable G^1 two-patch parameterizations. *Comput. Aided Geom. Des.*, 52–53:75 – 89, 2017.
- [22] M. Kapl, G. Sangalli, and T. Takacs. Isogeometric analysis with C^1 functions on unstructured quadrilateral meshes. Technical Report 1812.09088, arXiv.org, 2018.
- [23] M. Kapl, G. Sangalli, and T. Takacs. An isogeometric C^1 subspace on unstructured multi-patch planar domains. *Comput. Aided Geom. Des.*, 69:55–75, 2019.
- [24] M. Kapl and V. Vitrih. Space of C^2 -smooth geometrically continuous isogeometric functions on planar multi-patch geometries: Dimension and numerical experiments. *Comput. Math. Appl.*, 73(10):2319–2338, 2017.
- [25] M. Kapl and V. Vitrih. Space of C^2 -smooth geometrically continuous isogeometric functions on two-patch geometries. *Comput. Math. Appl.*, 73(1):37 – 59, 2017.
- [26] M. Kapl and V. Vitrih. Dimension and basis construction for C^2 -smooth isogeometric spline spaces over bilinear-like G^2 two-patch parameterizations. *J. Comput. Appl. Math.*, 335:289–311, 2018.
- [27] M. Kapl and V. Vitrih. Solving the triharmonic equation over multi-patch planar domains using isogeometric analysis. *J. Comput. Appl. Math.*, 358:385–404, 2019.

- [28] M. Kapl, V. Vitrih, B. Jüttler, and K. Birner. Isogeometric analysis with geometrically continuous functions on two-patch geometries. *Comput. Math. Appl.*, 70(7):1518 – 1538, 2015.
- [29] K. Karčiauskas, T. Nguyen, and J. Peters. Generalizing bicubic splines for modeling and IGA with irregular layout. *Comput.-Aided Des.*, 70:23 – 35, 2016.
- [30] J. Kiendl, E. Marino, and L. De Lorenzis. Isogeometric collocation for the Reissner-Mindlin shell problem. *Comput. Methods Appl. Mech. Engrg.*, 325:645–665, 2017.
- [31] E. Marino, J. Kiendl, and L. De Lorenzis. Explicit isogeometric collocation for the dynamics of three-dimensional beams undergoing finite motions. *Comput. Methods Appl. Mech. Engrg.*, 343:530–549, 2019.
- [32] M. Montardini, G. Sangalli, and L. Tamellini. Optimal-order isogeometric collocation at Galerkin superconvergent points. *Comput. Methods Appl. Mech. Engrg.*, 316:741–757, 2017.
- [33] B. Mourrain, R. Vidunas, and N. Villamizar. Dimension and bases for geometrically continuous splines on surfaces of arbitrary topology. *Comput. Aided Geom. Des.*, 45:108 – 133, 2016.
- [34] T. Nguyen and J. Peters. Refinable C^1 spline elements for irregular quad layout. *Comput. Aided Geom. Des.*, 43:123 – 130, 2016.
- [35] J. Peters. Geometric continuity. In *Handbook of computer aided geometric design*, pages 193–227. North-Holland, Amsterdam, 2002.
- [36] A. Reali and T. J. R. Hughes. An introduction to isogeometric collocation methods. In *Isogeometric Methods for Numerical Simulation*, pages 173–204. Springer, 2015.
- [37] D. Schillinger, M. J. Borden, and H. K. Stolarski. Isogeometric collocation for phase-field fracture models. *Comput. Methods Appl. Mech. Engrg.*, 284:583 – 610, 2015.
- [38] D. Schillinger, J. A. Evans, A. Reali, M. A. Scott, and T. J.R. Hughes. Isogeometric collocation: Cost comparison with Galerkin methods and extension to adaptive hierarchical NURBS discretizations. *Comput. Methods Appl. Mech. Engrg.*, 267:170 – 232, 2013.
- [39] D. Toshniwal, H. Speleers, R. Hiemstra, and T. J. R. Hughes. Multi-degree smooth polar splines: A framework for geometric modeling and isogeometric analysis. *Comput. Methods Appl. Mech. Engrg.*, 2016.
- [40] D. Toshniwal, H. Speleers, and T. J. R. Hughes. Analysis-suitable spline spaces of arbitrary degree on unstructured quadrilateral meshes. Technical Report 16, Institute for Computational Engineering and Sciences (ICES), 2017.

- [41] D. Toshniwal, H. Speleers, and T. J. R. Hughes. Smooth cubic spline spaces on unstructured quadrilateral meshes with particular emphasis on extraordinary points: Geometric design and isogeometric analysis considerations. *Comput. Methods Appl. Mech. Engrg.*, 327:411–458, 2017.